Prediction of pro-arrhythmic activity in humans with the use of physiologically based pharmacokinetics and pharmacodynamics modelling

A thesis submitted for the degree of Doctor of Philosophy

September 2018

Nikunjkumar K Patel

Faculty of Pharmacy

Jagiellonian University Medical College, Krakow, Poland

Supervisor: Dr hab. Sebastian Polak

Co-supervisor: Dr. Barbara Wiśniowska

Contents

Abstract

Drug induced cardiac arrhythmia, especially occurrence of Torsade de Pointes (TdP), has been a leading cause of attrition and post-approval re-labelling and withdrawal of many drugs. TdP is a multifactorial event, reflecting more than just drug-induced cardiac ion channel inhibition and QT interval prolongation. A drug that is well tolerated in most patients can cause TdP in a particular individual under certain clinical situations e.g. disease or co-medications or electrolyte imbalance. Moreover, assessment of the TdP liability of a drug based only on the parent moiety and the hERG (**h**uman ***E**ther-à-go-go*-**R**elated **G**ene) centric evaluations could be misleading since many drugs such as citalopram affect not only rapidly activating delayed rectifier potassium current (I_{Kr}) but also other ionic currents and may have electro-physiologically active metabolites. Testing all probable hypotheses in clinical and/or animal studies may be practically, ethically and economically unfeasible. In addition relating findings from animal studies to humans can be flawed due to species-specific differences in pharmacokinetics (PK) and toxicological response. These present a translational gap in extrapolating preclinical cardiac safety assessment to estimate human TdP risk reliably, especially when the drug of interest is used in combination with other QT prolonging drugs for treatment or has active metabolites. Thus, novel translational tools that allow prediction of clinical cardiac toxicity risk and expected clinical QT prolongation response are greatly needed. One such set of tools are physiologically based, biophysically detailed models of cardiac physiology that can characterize the contributions of multiple ion channel inhibition on the electrophysiology of human cardiomyocytes incorporated in the physical model of ventricular wall as string of cells arranged from inside to outside of ventricular wall. As part of this thesis, it was demonstrated with case examples how such mechanistic approach can be used from early discovery to late stage drug development and post marketing surveillance safety assessment where the model in enriched as more knowledge about the PK and safety of the drug becomes available. In early discovery, such Quantitative Systems Toxicology and Safety (QSTS) models can be run with properties predicted from chemical structure to aid high throughput virtual screening or prioritization of promising molecules and as more *in vitro* and clinical data becomes available, the models can be further verified, refined and enriched by "predict-learn-confirm" process. Prior simulations of clinical thorough QT trial for example could help reduce, refine or optimize the clinical study design to reach meaningful endpoint and help reduce the chance of study failure. With the case studies of moxifloxacin, citalopram and tolterodine, the utility of such QSTS approach to build and test hypothesis was demonstrated, such as (1) assessing the role of plasma versus heart tissue concentration in driving the cardiac response; (2) assessing the contribution of electro-physiologically active metabolite; (3) understanding impact of population variability such as genetic polymorphism on the cardiac safety profile of drugs: (4) impact of drug effect on cardiac ion channels other than hERG on cardiac safety of drug and (5) personalized safety assessment by simulating "virtual twin" of a real patient *in silico*. Adoption of such QSTS modelling strategies from early stages of drug discovery and development and enrichment of model and information along with drug product life cycle could allow bridging translational gap in clinical cardiac safety assessment.

Declaration

No portion of this work referred to in this thesis has been submitted in support of an application for another degree or qualification of this or any other university of other institute of learning.

Copyright Statement

Dedication

To my lovely wife Ankita and darling daughter Nikita, for your unconditional support and love during demanding last six years

To my mother Indiraben, an inspiration and a pathfinder

To my late father Kanaiyalal who inculcated scientific curiosity in me

I hope I can make you all proud

Acknowledgements

First, I would like to convey my deepest gratitude to my mentor, friend, colleague Dr. hab Sebastian Polak for encouraging me to pursue my PhD as an external student. It was his support; guidance and constant encouragement that helped me push myself to pursue this dream. Apart from extending his scientific knowledge in cardiac safety research field, he had always been there in tough time to help me focus and in good times to celebrate. I cannot imagine writing this thesis without his guidance and support.

I would like to thank Simcyp Limited, now Certara UK Limited, and my employer of last seven years, for extending their full support to pursue my external doctoral studies.

I would like to convey my sincere gratefulness to my co-mentor, Dr. Barbara Wisniowska for extending help and guidance when I needed throughout the duration of the studies.

Ms. Zofia Tylutki, it would have been tough to pursue my studies being external student in another country without a friend like you at the university always ready to help, thank you.

My sincere thanks to the Jagiellonian University Medical College and the faculty for allowing me enrol as external PhD student and warmest welcome extended to me as a student whenever I visited the university.

An infinite gratitude to my wife Ankita and daughter Nikita, this would not have been possible without your constant love, encouragement, support and dedication. Thank you for allowing all the time needed that I might have stolen from weekends and evenings. To my beloved mother and late father, thank you for your inspiration and blessings.

List of Contributed Publications

This thesis is based research findings reported in following peer-reviewed publications (sorted chronologically starting with most recent) for which permissions were obtained for reprints from the respective publishers to include in the thesis. The reprints of the original publications are appended at end of this thesis.

P-I. **Patel N**, Wisniowska B, Polak S. *Virtual Thorough QT (TQT) Trial-Extrapolation of In Vitro Cardiac Safety Data to In Vivo Situation Using Multi-Scale Physiologically Based Ventricular Cell-wall Model Exemplified with Tolterodine and Fesoterodine*. AAPS J. 2018 Jul 11;20(5):83. doi: 10.1208/s12248-018-0244-3. (5-year Impact Factor 4.911; MNiSW 40)

P-II. **Patel N**, Hatley O, Berg A, Romero K, Wisniowska B, Hanna D, Hermann D, Polak S. *Towards Bridging Translational Gap in Cardiotoxicity Prediction: an Application of Progressive Cardiac Risk Assessment Strategy in TdP Risk Assessment of Moxifloxacin*. AAPS J. 2018 Mar 14;20(3):47. doi: 10.1208/s12248-018-0199-4. (5-year Impact Factor 4.911; MNiSW 40)

P-III. **Patel N**, Wiśniowska B, Jamei M, Polak S. *Real Patient and its Virtual Twin: Application of Quantitative Systems Toxicology Modelling in the Cardiac Safety Assessment of Citalopram*. AAPS J. 2017 Nov 27;20(1):6. doi: 10.1208/s12248-017-0155-8. (5-year Impact Factor 4.911; MNiSW 40)

P-IV. Fijorek K*, **Patel N***, Klima Ł, Stolarz-Skrzypek K, Kawecka-Jaszcz K, Polak S. *Age and gender dependent heart rate circadian model development and performance verification on the proa+rrhythmic drug case study*. Theor Biol Med Model. 2013 Feb 9;10:7. doi: 10.1186/1742-4682-10-7. (5-year Impact Factor 1.308; MNiSW 25)

* Joint first authorship

Abbreviations

QSTS	Quantitative Systems Toxicology and Safety
PBPK	Physiologically-Based Pharmacokinetic (Model)
PK	Pharmacokinetics
PD	Pharmacodynamics
ECG	Electrocardiogram
QT	Is the time interval between Q and T wave on ECG trace
RR	Time interval between two consecutive R waves on ECG
HR	Heart rate
QTc	QT interval corrected by heart rate
ΔQTc	QTc interval prolongation by drug with respect to baseline
ΔΔQTc	QTc interval prolongation by drug with respect to baseline and placebo
QTcF	QT interval corrected for heart rate using Fridericia formulae
hERG	**h**uman ***E****ther-à-go-go*-**R**elated **G**ene
TQT	Thorough QT/QTc trial
TdP	Torsade de pointes
IND	Investigational new drug
XO	Xenopus Oocytes
CHO	Chinese Hamster Ovary
HEK	Human Embryonic Kidney
CiPA	Comprehensive *in Vitro* Pro-arrhythmia Assay
QSAR	Quantitative structure activity relationship
FAERS	FDA Adverse Event Reporting System
I_{Kr}	rapidly activating delayed rectifier potassium channel current
I_{Ks}	slowly activating delayed rectifier potassium channel current
I_{Na}	Sodium current
I_{CaL}	Late calcium current
IC_{50}	Concentration of the ligands required to inhibit 50% of the current of studied ion channel
N	Hill coefficient
C_{max}	Maximum plasma drug concentration
$C_{max,ss}$	C_{max} at steady state after multiple dosing

1. Introduction

Cardiac toxicity is one of the leading causes of high attrition rate at various stages of drug development, withdrawal of several marketed drugs and extensive relabelling of many drugs (1-4). Among various types of cardiotoxic effects, arrhythmogenicity is one of the most common post-approval adverse event (3). Risk of occurrence of the life-threatening Torsades de Pointes (TdP) arrhythmia degenerating into the ventricular fibrillation, is assessed generally by QT interval prolongation liability – considered, yet not without criticism, a TdP risk surrogate (5, 6). The risk of TdP has been ascribed for drugs spanning wider therapeutic areas, other than cardiovascular drugs (7); hence, it has become important to assess the TdP risk for any new medicine. Due to the potentially significant safety impact and corresponding regulatory concern of drug-induced cardiotoxicity, careful assessment of pro-arrhythmic potential is an integral part of preclinical and clinical safety evaluation of an investigational new drug (IND). There are several methods and protocols available for assessment of drug's proarrythmic potential spanning from *in silico*, *in vitro*, *ex vivo*, *in vivo* animal to dedicated clinical trial to answer the set of questions asked about cardiac safety at various stages of drug development. The most commonly utilised pathways at non-clinical stage of development include *in vitro* models where the human ion channels involved in cardiac electrophysiology are heterologously expressed in non-human (e.g., Xenopus Oocytes – XO and Chinese Hamster Ovary – CHO cells) and human (e.g., Human Embryonic Kidney – HEK cells) cell lines and used for assessment of the drug triggered ionic currents inhibition (8). These approaches continue to evolve, with newer approaches such as the Comprehensive *in Vitro* Pro-arrhythmia Assay (CiPA) initiative, assessing i.e. the role of stem-cell derived cardiomyocytes in cardiac safety assessment (6-10).

With the advancement of machine learning techniques in the field of life sciences, various quantitative structure activity relationship (QSAR) models that are sufficiently trained and properly validated are increasingly being employed to predict new chemicals activity towards the ionic currents inhibition either to reduce the *in vitro* experiments or to fill data gaps in preclinical safety profiling of the new drugs (9-14). Sometimes, more time and resource intensive *ex vivo*/*in vivo* animal studies in monkeys, rabbits, dogs or guinea pigs are performed to study drug effect at cardiac level after oral or systemic drug administration (15-17). At the clinical level, Thorough QT/QTc (corrected QT) (TQT) trials are introduced to assess relative QT prolongation by candidate drug as compared to placebo and positive control (5). In 2005,

the ICH issued a first formal guidance (E14) in this regard – "The Clinical Evaluation of QT/QTc Interval Prolongation and Proarrhythmic Potential for Non-Antiarrhythmic Drugs". QTc is the QT interval of ECG profile corrected for the heart rate variations by suitable formulae. The major aspect of the guidance was the Thorough QT/QTc (TQT) study that is a dedicated and well-controlled clinical trial to quantify the propensity of drug to prolong QT/QTc at therapeutic and supra-therapeutic dose levels as compared to positive control and placebo. The cause of concern in TQT trial is the QT prolongation exceeding 5 ms determined by whether the upper boundary of the 95% confidence interval around the mean effect on the QT interval is larger than 10 ms. QT interval varies significantly larger than 5 ms naturally during the day, due to physical activity rate, metal stress, circadian rhythms, meal intake, gender and hormonal effects and multiple other factors; hence to detect such a small difference in a parameter (QT interval) with inherently high basal variability, the study is typically well controlled for baseline, placebo, time of day (circadian) effects and includes positive control (typically moxifloxacin (MOXI)). QT varies with heart rate hence various correction formulae are applied to correct QT for heart rate changes (known as QTc) among which Fridericia method is widely used (18). E14 guidelines are adopted by many regulatory agencies and TQT trials have become routine in new drug approval process. There are some rules of thumb and decision trees available to qualitatively (yes/no) predict clinical QT prolongation in humans or at best to guide type of assays to be carried out at next level of assessment (19-21).

Despite the availability of multiple models and the continued advances in cardiac risk assessment, the number of reports of TdP remains significant (over 100 cases of the TdP reported to the FDA Adverse Event Reporting System (FAERS) every year) and almost half of them are related to non-cardiovascular drugs (4, 7, 22). This reflects a translational gap in the quantitative clinical extrapolation from the typical cardiac safety data collected, such as early non-clinical drug screens for cardiac ion channel inhibition, particularly hERG (**h**uman ***E****ther-à-go-go*-**R**elated **G**ene) inhibition, or the propensity for QT interval prolongation as assessed in early phase and TQT clinical trials to the actual occurrence of TdP event in clinical practice. Consequently, to minimize TdP risk under an optimized drug development paradigm, early stage gates are often employed which only progress compounds predicted or observed to have little to no increase in QT interval, raising concerns that therapeutically promising agents may be triaged inappropriately. These concerns represent findings that the occurrence of TdP is multifactorial, reflecting more than just a drug's ability to inhibit hERG or increase the QT interval. These additional factors, such as gender, co-medications, comorbidities and genetic

polymorphisms, make a drug which is relatively safe for most people under controlled clinical trials and routine clinical practice potentially cardiotoxic for a few individuals under specific circumstances (23). Thus actual incidence of TdP can be a result of multiple clinical risk factors other than drug's ability to perturb cardiac electrophysiology making it rare and challenging to predict its risk precisely. However, as TdP is a type of polymorphic ventricular tachycardia or arrhythmia, there is an association between prolongation of QT interval of ECG and TdP. A drug that can prolong QT interval could potentially cause TdP. Hence, QT interval prolongation by the drug is considered an acceptable biomarker of TdP risk albeit with some criticism (24).

Moreover, the assessment of torsadogenic potential of a drug based only on parent drug and only hERG inhibition activity could be misleading as many drugs affect ionic currents other than I_{Kr} (rapidly activating delayed rectifier potassium current, mainly governed by the hERG gene coded ion channel, is crucial for repolarization of cardiac action potentials) and may have electro-physiologically active metabolites. Animal studies may not be a good surrogate in such situations as there are known physiological differences in drug absorption, distribution and metabolism between animals and humans along with cardiac (electro-) physiology variations (25). Testing all permutations and hypotheses in clinical studies are ethically and economically infeasible during clinical development which has led to some of the approved drugs being withdrawn from the market due to identification of considerable TdP events associated drugs only in post-marketing surveillance when the drug has been administered to wider range of subjects and situations (e.g., co-medications, disease and environmental factors) as compared to controlled clinical trial environment.

Translational tools with improved predictive performance that account for the multi-factorial determinants of cardiotoxicity, particularly TdP, are needed to improve both the cardiac risk assessment and attrition rates of compounds in development. One such set of tools are physiologically based, biophysically detailed models of cardiac physiology that can characterize the contributions of multiple ion channel inhibition on the electrophysiology of human cardiomyocytes. Such models could be categorized under a broader category termed as QSTS (Quantitative Systems Toxicology and Safety) modelling (23). Such multi-scale QSTS models can bridge the translational gap in cardiac safety assessment during the early drug development stage by faithfully reproducing the mechanistic exposure-response relationships from the molecular level to the full organism level. Specifically, simulations using this framework can link predicted or observed drug pharmacokinetics (PK) via physiologically based PK (PBPK) modelling with dynamic ion channel inhibition and subsequent effects on

ECG matrices in virtual patients, which represent an array of physiologies (23, 26-28). When supported with the database of human physiological variability both within subject and between subjects variability, such mechanistic QSTS models allow the possibility to simulate ECG based on *in vitro* cardiac safety data identifying the high-risk clinical scenarios to inform safe use of drugs (22).

The Cardiac Safety Simulator (CSS) platform (Certara UK Limited, Sheffield, UK) (29), previously known as ToxComp platform (30), incorporates electrophysiology models of ventricular cardiomyocytes and can simulate the tissue level response such as pseudoECG (ECG profile without the P wave, which is characterised by the atrial activity) by simulating the conductance of current across ventricular wall thickness with the use of string of cardiomyocyte cells in series. However, to relate the pseudoECG to clinically measured ECG profile, the model needed to include the aspect of inherent population variability on ECG profile. Hence, circadian model of heart rate as covariate of age and gender was introduced to be able to simulate the circadian and inter-individual variability in heart rate (RR interval of ECG profile) that could allow better simulation of clinical reality (**Publication P-IV**). The covariate model of heart rate was developed and verified for predictive performance mathematically as well as in terms of predicting the actual QT interval prolongation reported for most widely used positive control drug MOXI.

As part of the research reported in this thesis, a QSTS model based strategy for progressive cardiac risk assessment was proposed and verified, where the risk assessment for a novel compound is refined progressively as clinical knowledge is enriched through predict-learn-confirm cycles (**Publication P-II**) (23). The individual model components are iteratively verified/refined, to reduce uncertainty and increase confidence, making them adaptable to more adequately address questions around therapeutic performance, as they arise during clinical development. The single cell simulation based Cardiac Risk Assessment as proposed by Abbasi *et al*. can be employed as high-throughput early discovery virtual screening or prioritization tool on large library of compounds (31). During lead optimization or early drug development, more refined cardiac risk stratification algorithm as proposed by Polak *et al.* that accounts for various clinical end points and estimated exposure levels can help assign the risk (low, moderate, high) to drug molecule and could help prioritize promising molecules to progress further or establish the risk benefit balance of individual compounds to make informed decisions for further development (28).

Figure 1. Progressive Cardiac Risk Assessment Strategy in TdP risk assessment

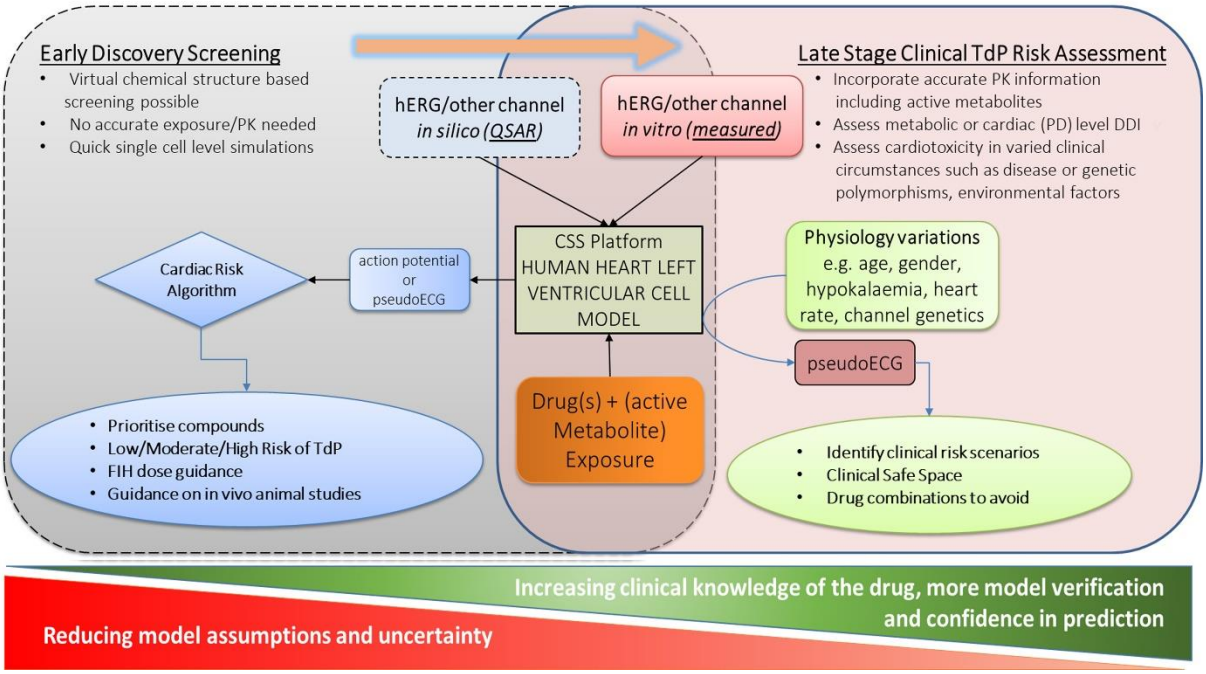

Such stratification methods can be particularly informative during early phase development to estimate potential cardiac safety risk even in the absence of detailed information about human PK and pharmacodynamics (PD), as sensitivity analyses maybe performed to simulate a range of possible clinical scenarios. As more PK and PD information about the drug becomes available with further drug development, these initial predictions can be verified and refined, and ultimately may be superseded by a more detailed PBPK-QSTS model platform where verified PBPK model could help estimate the exposure at site of action (heart tissue) and allow comparison of plasma versus heart tissue exposure and role of metabolites. Once sufficiently verified, the established and enriched model can be used to simulate clinical scenarios to evaluate effects of intrinsic and extrinsic factors (i.e., special populations, drug-drug interactions, co-morbidities) to establish the clinical cardiac risk scenarios [Figure 1]. This is demonstrated with example of MOXI where the drug is not leading to TdP even at 10-fold higher exposure in healthy cardiac physiology but could lead to abnormal pseudoECG when the same dose is given to subjects with modified heart rate and hypokalemia (23, 28). Such PBPK-QSTS approach could allow identification of high risk clinical scenarios and allow more suitable labelling of drug product or personalized therapy by appropriately avoiding the drug in high risk patients or clinical scenarios e.g. drug-drug interactions. Further, such PBPK-QSTS approaches can also be used for post-marketing surveillance and support patient monitoring

during hospitalization. Such utility was demonstrated by creating virtual twin of real patients for four different cardiac toxicity case reports of citalopram (CT) where the model was able to accurately simulate the QT prolongation observed in real patients at therapeutic and up to 100-fold higher exposure levels with various additional risk factors such as hypokalemia, bradycardia, tachycardia, etc. (**Publication P-III**) (26). It was a proof of concept that when suitably parameterized such QSTS modelling has strong potential for personalized safety assessment and monitoring. Using the case examples of tolterodine (TOL) and fesoterodine (FESO), the ability of such QSTS approach to simulate a clinical thorough QT trial was assessed and established (**Publication P-I**) (27). Such virtual TQT trial simulations prior to actual clinical study could help optimize, refine or avoid the clinical study. Application of a progressive PBPK-QSTS cardiac risk assessment paradigm starting in early development could guide drug development decisions and later define a clinical safe space for post-approval risk management to identify high-risk clinical scenarios.

2. Objectives

The main objective was to propose a cardiac safety risk assessment strategy that can be employed from early discovery and can be enriched progressively as more knowledge about the new drug becomes available in drug development life cycle to post-marketing surveillance supported with case studies to exemplify employment of such strategy for practical use. There were three major elements of the project:

- ✓ During the initial stages of the project, it was realised that simulation of clinical cardiac safety mostly assessed with ECG profile and QT interval prolongation would require ability of the QSTS model to mimic the circadian variability in heart rate including gender effect. Thus, the aim was to develop a physiological covariate model for circadian variability in heart rate with age and gender effects and to verify the ability of the model to accurately simulate the circadian variations in QT interval prolongation by most widely used positive control for TQT trials, moxifloxacin (**Publication P-IV**) (32).
- ✓ Define mechanistic modelling based framework for screening and prioritization of promising molecules in early discovery stage and identification of clinical safe space or high risk clinical situations in late development stage (**Publication P-II**) (23). The framework was also aimed to reduce, refine and optimize the clinical studies and study designs by prior simulations of virtual populations such as TQT trials (**Publication P-I**) (26). The mechanistic framework can be employed in post-marketing surveillance to understand or hypothesize mechanisms of toxicity event in particular patients by simulating virtual "*in silico*" twin of real patient (**Publication P-III**) (26). Each of these components were supported by case examples.
- ✓ Third major objective was to show with examples the importance of electro-physiologically active metabolites in cardiac risk profile of the parent drug. Most current early screening is focused on parent drug itself including that under the CiPA initiative while for many drugs metabolites could play important role. Comprehensive mechanistic modelling platforms such as CSS allows simulations of multiple moieties affecting one or more cardiac ion channels thus could help bridge such gap in safety assessment. The role of metabolites was studied for CT and TOL where the metabolite could increase the cardiotoxicity of parent drug (e.g. CT) or could mitigate the cardiotoxicity of parent (e.g. TOL).

3. Materials and Methods

3.1. Data to develop and verify the circadian model of heart rate

Development and verification of circadian model for heart rate changes for north European Caucasian population was published in **Publication P-IV**. This section provided the data used and methodology used for the study.

3.1.1. PhysioNet data set description

The analysed data set was obtained from the PhysioBank, which is an archive of digitized sets of data reflecting physiological signals. The data warehouse contains over 50 various freely available databases, and for modelling purposes the MIT-BIH Normal Sinus Rhythm Database was used (33). There were a total of 18 subjects, 5 males (average age 36, range 26–45) and 13 females (average age 34, range 20–50). For each subject up to 24 hours of RR interval recordings were available. Subjects, on average, had 94440 individual RR measurements (range 73300 – 115900). In order to decrease the significant computational burden it was necessary to reduce the number of RR measurements per subject. RR averaging in one-hour, half-hour and 15-minute 'time windows' was found inadequate due to its variability reduction property. Stable results were obtained after sampling RR measurements every 1 minute.

3.1.2. Validation data set

Model validation was performed with the use of a completely independent data set. Data was derived from Cracow's clinical research database (1st Department of Cardiology and Hypertension, Jagiellonian University Medical College). There were a total of 67 healthy subjects in the validation data set, 34 males and 33 females (average age 33, range 17–72). Validated oscillometric SpaceLabs 90207 monitors (Redmond, WA, USA) fitted with the appropriate cuff size were programmed to obtain readings every 15 minutes from 08.00 to 22.00 and every 30 minutes from 22.00 to 08.00. Each reading included systolic/diastolic blood pressure, mean arterial pressure and heart rate. Subjects, on average, had 71 heart rate measurements (range 35–99). RR interval length was calculated based on the heart rate measurement results.

3.1.3. Model usability testing

To test the usability of the implemented circadian rhythm model within the ToxComp platform, MOXI, the most commonly used positive control in TQT studies was chosen as the model

compound. The ToxComp system (now known as the CSS platform) was used to simulate the drugs triggered ECG modification. The ToxComp platform combines a physiologically based electrophysiological model of human left ventricular cardiomyocytes (ten Tusscher 2006 – TT2006) and a database of human physiological, genotypic and demographic data enabling the prediction of the QT prolongation in humans based on the *in vitro* data (34). To account for the heterogeneities in ionic currents between endocardial, midmyocardial and epicardial cells 1D fibre paced at the endocardial side was constructed. The 50:30:20 distribution of the endo-, mid- and epicardial cells was used together with a diffusion coefficient equal to 0.0016 cm2/ms. The Forward Euler method was used to integrate model equations. Integration results were used to calculate a pseudo-ECG. First and last QRS were excluded from the pseudo-ECG. A space step and a time step were set to Δx=0.01 mm and Δt=0.01 ms, total simulation time was set to 10000 ms.

To account for the drugs triggered ionic currents modifications a specific equation describing the current of interest was multiplied by the inhibition factor accordingly to the *in vitro* values provided by the literature search, which described the concentration dependent ionic current inhibition. The inhibition factor was calculated with the use of the Hill equation [Equation 1].

$$Inhibition\ Factor = \frac{1}{1+(IC_{50}/[D])^{n}} \qquad \text{[Eq. 1]}$$

where IC_{50} – concentration responsible for the 50% inhibition of the ionic current; n – Hill equation parameter; [D] – active drug concentration [μM]

The population variability of other parameters was mimicked by applying the virtual population generator as described previously (35, 36). The circadian heart rate variability was introduced into a simulation by the use of the developed covariate circadian model.

3.8 μM of MOXI was used as the operational concentration, mimicking the average maximum free plasma concentration ($C_{max,free}$) after a 400 mg oral dose by correcting the total C_{max} concentration obtained from the available literature with human plasma protein binding (37, 38). The IC_{50} values for various cardiac ion channels were obtained from the tox-database.net system (39). For the simulation studies only I_{Kr} IC_{50} of 29μM (40) data was used (with Hill equation coefficient n = 1) since for the tested MOXI concentration I_{Na} (sodium current) and I_{CaL} (late calcium current) inhibition were negligible.

The ToxComp simulations, at a MOXI concentration equal to $C_{max,free}$ at different times of the day (4.00, 8.00, 12.00, 16.00, 20.00, and 24.00), were performed in triplicate trials of 20 individuals (total 3×20=60) with an equal number of male and female subjects in each trial. Baseline QT and QTcF (QT interval corrected by heart rate using Fridericia correction method (18)) were also obtained for each subject at the above defined time points of the day by simulating a response at MOXI concentration equal to zero. This allowed us to apply two baseline correction formulas i.e., (1) Single point baseline correction when the average baseline QTcF estimates from all subjects was used to obtain baseline corrected QTcF (ΔQTcF) and (2) Individualised baseline correction ($\Delta QTcF_i$) when baseline QTcF at a given time of day for each individual subject was used to calculate ΔQTcF. The developed circadian effect model was validated by comparing the simulated results with respective clinical outcomes obtained using single point and individualized baseline correction formula.

3.2. Data to develop and verify virtual TQT trial simulation model

The research work on virtual TQT trial was published in **Publication P-I**. Input data and methodology used in development and verification of virtual TQT model is described in this section.

3.2.1. Pharmacology of the tested drugs

5-hydroxymethyl tolterodine (5-HMT) is formed by metabolism of TOL via cytochrome P450 (CYP) 2D6 enzyme (41, 42), which is known to have genotypic and phenotypic differences in human populations (43). 5-HMT itself is metabolised predominantly via CYP2D6 and CYP3A4 pathways with minor contribution of renal excretion. The clinical TQT study (41) identified the extensive metaboliser (EM) and poor metaboliser (PM) phenotype status of subjects and reported the exposure levels for both EM and PM groups and the subsequent QT prolongation. Natural frequency of PM phenotype in Caucasian population is around 8% (Simcyp in-house meta-analysis data). However, the clinical study recruited around 45% subjects with PM status to include sufficient representation of PM group in the studied cohort. EM and PM groups with number of subjects as defined in the clinical study were simulated and the predictions were verified with the clinical data. The influence of exposure in systemic circulation versus estimated exposure in heart tissue was also studied.

FESO is an ester pro-drug of 5-HMT. FESO was designed to produce therapeutically active metabolite (5-HMT) of TOL avoiding the CYP2D6 polymorphism related variability in

pharmacokinetics in exposure levels in patients because the conversion of FESO to 5-HMT is driven by ubiquitous esterase enzymes (44). FESO converts rapidly and almost completely to 5-HMT in systemic circulation as evident from the observation that the FESO is almost undetectable in systemic circulation after oral administration (45).

3.2.2. Clinical PK and QT prolongation data

3.2.2.1. Tolterodine

Bio-relevant exposure levels of active chemical moieties along with ion channel activity are required as input to the CSS system to predict the QT interval prolongation effect. Malhotra *et al.* (41) have reported results from a TQT trial at therapeutically recommended (2 mg BID) and supra-therapeutic (4 mg BID) dose of TOL with 400 mg MOXI as positive control. The steady state (day 4) maximum plasma concentration ($C_{max,SS}$) for TOL and metabolite 5-HMT after 2 mg and 4 mg bid dose levels for CYP2D6 EM and PM subject groups along with $C_{max,SS}$ for MOXI treatment were obtained from Malhotra el al. (41). Virtual subjects were generated based on the demographic information (age, gender, and body weight) provided in the clinical study based on bootstrapping method. The population variability in drug exposure parameters (here $C_{max,SS,TOL}$ and $C_{max,SS,5\text{-}HMT}$ for both EM and PM groups) was simulated using the bootstrapping method based on the mean and variance of population PK parameters reported in the study. The population variability in PK was then propagated into the CSS platform to predict the QT prolongation for the virtual trial population. The placebo effect was simulated as the QT prolongation response with zero drug concentration for a given subject at given time point. Heart tissue to plasma partition coefficient ($K_{heart:plasma}$) was estimated with 'Method 3' in Simcyp simulator V16 (Certara UK Limited, Sheffield, UK) where the 'bottom-up' predicted volume of distribution at steady state (V_{ss}) from physicochemical parameters of the chemical moieties was calibrated with observed V_{ss} for both TOL and 5-MHT using 'Kp scalar'. 'Kp scalar' is a multiplier to the estimated tissue:plasma partition coefficients from 'Method 3' of Simcyp simulator. The observed V_{ss} for TOL was 1.66 L per kg of body weight (46) while the predicted V_{ss} from 'Method 3' from physicochemical parameters was 2.8 L/kg. With 'Kp scalar' value of 0.75 the predicted V_{ss} matched well to the observed V_{ss}. With adjusted 'Kp scalar' to match the observed V_{ss}, the estimated $K_{heart:plasma}$ for TOL was 0.48 and the fraction unbound in the heart tissue ($f_{u,Heart}$) from 'Method 3' was 0.066. Similarly, the 'Kp scalar' for 'Method 3' was adjusted to 0.46 to match the observed V_{ss} of 1.73 L/kg for 5-HMT (47). With adjusted 'Kp scalar' to match the observed V_{ss}, the estimated $K_{heart:plasma}$ for 5-HMT was 2.93 and the $f_{u,Heart}$ from 'Method 3' was 0.088. These estimated values of $K_{heart:plasma}$ and

the $f_{u,Heart}$ for TOL and 5-HMT were used to calculate the total and unbound heart tissue concentration of both moieties from the observed plasma concentration data.

3.2.2.2. Moxifloxacin

Daily dose of 400 mg MOXI was administered orally to volunteers in positive control arm of the TQT trial and QT prolongation was estimated on day 4. A PBPK-QSTS model for MOXI was previously developed and verified (23). The same PBPK model of MOXI was used and ran simulation for multiple daily dose of 400 mg and calculated the maximum unbound heart tissue exposure levels on day 4 and input to the CSS platform to drive the QT response. The maximum QTc prolongation was calculated from simulated study arm and compared with the reported QTcF prolongation in the TQT study report.

3.2.2.3. Fesoterodine

Malhotra *et al.* (45) have reported results from a thorough QT trial of FESO at therapeutically recommended (4 mg sustained release tablet once a day for three days) and supra-therapeutic (28 mg, seven sustained release tablets of 4 mg FESO given once a day for three days) dose of FESO with 400 mg MOXI as positive control. The steady state (day 3) maximum plasma concentration ($C_{max,SS}$) for active metabolite 5-HMT after 4 mg and 28 mg dose levels were obtained from Malhotra *et al*. (45). Similar to TOL, virtual subjects population variability in drug exposure parameters (here $C_{max,SS,5\text{-}HMT}$) were generated based on bootstrapping method. The population variability in PK was then propagated into the CSS platform to predict the QT prolongation for the virtual trial population. The placebo effect was simulated as the QT prolongation response with zero drug concentration for a given subject at given time point. Simulations with only unbound plasma concentration as operating concentration were studied for FESO.

3.2.3. In vitro/in silico cardiac safety data

TOL is known to inhibit at least three cardiac ion currents namely I_{Kr}, I_{Na} and I_{CaL} (sodium and late calcium currents respectively) that are important in cardiac electrophysiology (48). Its metabolite, 5-HMT, is also known to inhibit at least the same three cardiac ion channel currents as the parent albeit with different potency (48). Concentration of the ligands required to inhibit 50% of the current of studied ion channel (IC_{50} values) of TOL and 5-HMT for I_{Kr}, I_{Na} and I_{CaL} currents are reported in Table 1.

Table 1. Cardiac ion channel inhibition data used in simulations and its source

Moiety	IC_{50} in µM (Hill equation coefficient[$])			
	I_{Kr}	I_{Na}	I_{CaL}	Reference
TOL	0.011 (1)	4.85 (1)	560 (1)[*]	(48, 49)
5-HMT	0.39 (1)	17.25 (1)	560 (1)[^]	(48, 49)

**Calculated IC_{50} within the CSS platform based on %inhibition versus concentration profile reported in reference (17% inhibition at 15 µM concentration of TOL); ^Calculated IC_{50} within the CSS platform based on %inhibition versus concentration profile reported in reference (18% inhibition at 15 µM concentration of TOL); [$]Hill coefficient was not reported in the study hence assumed to be 1 in all cases; I_{Kr} – rapidly activating delayed rectifier potassium current; I_{CaL} - late calcium current and; I_{Na} – peak sodium current.*

3.3. Data to develop and verify moxifloxacin PBPK-QSTS model for late stage clinical question assessment

Simcyp Simulator V16 (Certara, Sheffield, UK) was used for PBPK simulations (50). The Advanced Dissolution, Absorption and Metabolism (ADAM) model was used to mechanistically simulate the formulation effects on drug absorption and 14 organ full body perfusion limited PBPK distribution model was used to model disposition after systemic absorption (51, 52). The recently established PBPK model parameters (Table 2) were used to simulate the pharmacokinetics of MOXI after oral administration and estimate the population variability in the lung tissue disposition (53), resulting in a mechanistic PK-PD model for translation of the *in vitro* cardiac safety assessment to clinical level. Poulin and Theil method (54) with Berezhkovskiy correction (55) was used to estimate the tissue:plasma partitioning of MOXI. This method under-predicted the volume of distribution in comparison to volume of distribution reported for MOXI after intravenous administration to human volunteers, hence the model was calibrated with 'Kp scalar' using Simcyp parameter estimation module.

Table 2. Parameter values input for the MOXI PBPK simulations using Simcyp.

Parameter	Value	References and notes
MW	401.4	(56)
Compound Type	Ampholyte	(57)
pKa1 (acidic)	6.25	(57)
pKa2 (basic)	9.29	(57)
Log$P_{o:w}$	7.8	(57)
fu (measured)	0.514	(58-61)
B:P (measured)	1.5	(62)
Absorption Model	ADAM	Advanced Dissolution Absorption and Metabolism
P_{app} Caco-2 (pH 7.4:7.4) ($x10^{-6}$ cm/s)	10.6	Passive + Active (63)
Intrinsic Solubility (mg/mL)	1.146	PubChem Database
Formulation type		Immediate Release tablet
Prandial State	Fasted	Fasted state physiology simulated for digestive tract
Distribution Model	Full PBPK	Poulin and Theil method (54) with Berezhkovskiy correction (55) [Simcyp Method 1]
K_p Scalar	4.22	Optimised using parameter estimation with intravenous dosing PK data (61)
V_{ss} (L/kg) – Predicted	1.82	Tissue:plasma Kp predicted with Method 1 (54, 55)
Total Plasma Clearance CL_{iv} (L/h)	12.56	Optimised using parameter estimation with intravenous dosing PK data (61)
CL_R (L/h)	2.72	(38, 59-61, 64-66)
		Renal elimination accounts for ~20% of dose.

LogPo:w Log of the octanol:water partition coefficient, fu fraction unbound in plasma, B:P Blood-to-plasma ratio, Kp partition coefficient, Vss volume of distribution at steady state, CL_R in vivo renal clearance.

The PBPK model derived concentration-time profiles for various bio-phases was used to drive the CSS pseudoECG response. The PBPK model was linked with the mechanistic cardiac QSTS model for MOXI. As the purpose of the study was to show application of the PBPK-QSTS framework in early clinical development, a Phase 1 healthy volunteer study was simulated. A virtual population of 20 healthy Caucasian individuals (50% female) aged 20-50

years old was used to simulate single-dose fasted-state administration of a 400 mg MOXI tablet formulation, similar in size to a positive control arm in a typical TQT trial. The resulting plasma concentration-time profiles were verified by comparison to the observed clinical PK data reported by Stass *et al*. (60). CSS model [Figure 2] considers the heterogeneities in ionic currents between endocardial, midmyocardial and epicardial cells by 1D fibre paced at the endocardial side.

Figure 2. Framework of CSS platform (A); and covariate models in the platform (B)

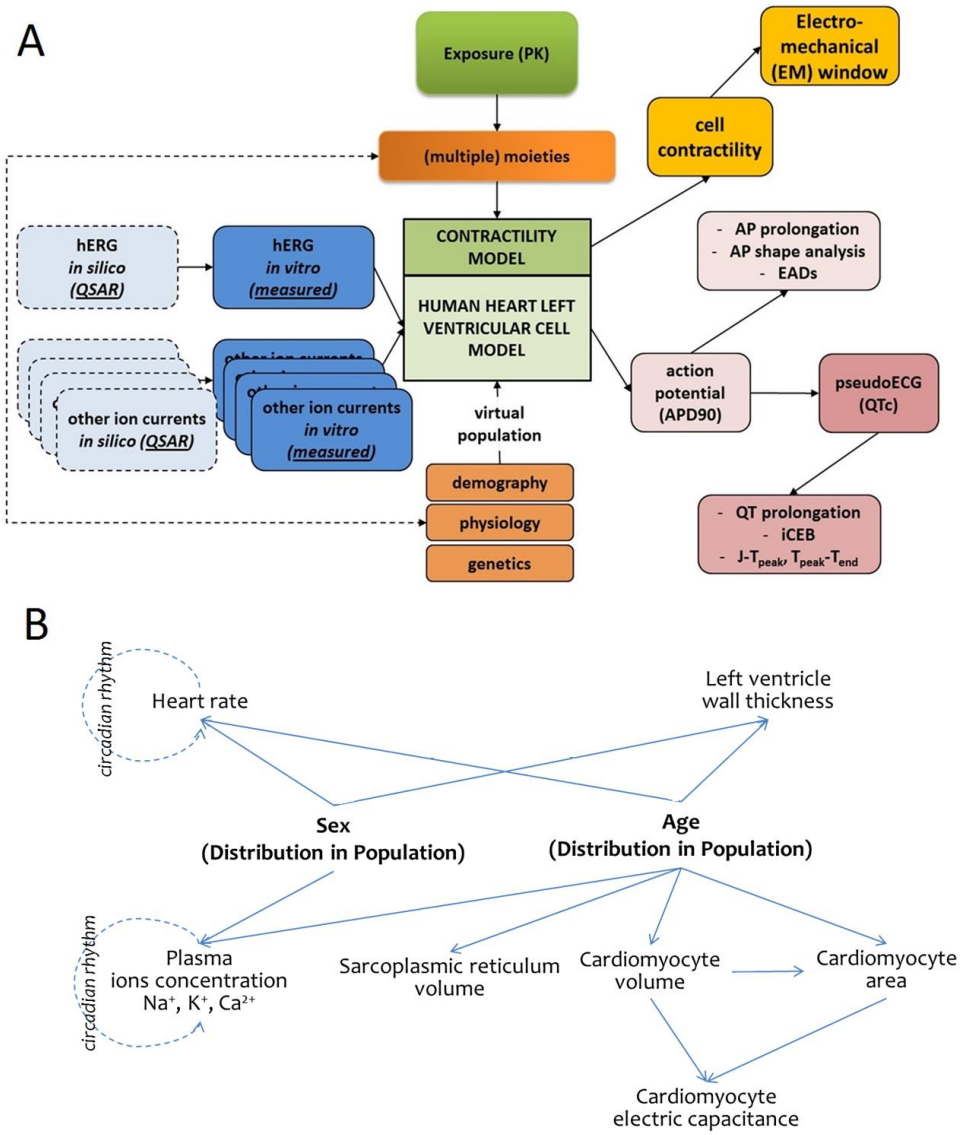

The population variability of other physiological parameters was mimicked by applying the virtual population generator as described previously (35, 36). The circadian heart rate variability

model has recently been incorporated into the CSS system to enable assessment of circadian variations in heart rate on the estimate of QT prolongation (32). To account for the circadian plasma ions variability model describing the gender dependent diurnal fluctuation of three main ions (Ca^{2+}, K^+ and Na^+) has been applied (67, 68). Epidemiological and covariate models which take into account the effect of gender and age on ventricular heart wall thickness, cardiomyocyte volume and capacitance, and sarcoplasmic reticulum volume are also built into the CSS platform for the north European Caucasian population with healthy heart physiology (30). The output from the CSS is in the form of a pseudo-electrocardiogram (i.e., a virtual ECG), including measures of interest (e.g., QRS, QT).

For this study, the CSS implementation of the ten Tusscher 2006 (TT2006) ventricular cardiomyocyte cell model (34) was used primarily to form a one-dimensional cardiomyocyte string mimicking the ventricular wall cross-section (thickness). The use of another widely used cardiomyocyte model, O'Hara and Rudy (ORd) model (69), was also assessed on the predicted pseudoECG.

For simulation of the effects of a compound on the pseudoECG outputs, the required model inputs are the *in vitro* measured IC_{50} values for relevant cardiac ion currents, operating drug exposure concentrations, time of day (clock time for circadian model) and age and gender of each simulated subject which can be directly read into the CSS platform from the Simcyp PBPK model output. MOXI's cardiac effects are primarily linked to I_{Kr}) inhibition, as effects on other currents, namely I_{CaL} and I_{Na}, show IC_{50} values many-fold higher than the operating physiological tissue concentrations of MOXI after 400 mg single-dose administration and were obtained from non-human cell systems. Hence only the inhibition of I_{Kr} by MOXI was considered in our simulations, with corresponding IC_{50} values obtained from the freely available tox-database.net (Table 3) (39). Consistent with other experiments in biological systems, there is considerable inter-laboratory variability in reported IC_{50} values for I_{Kr} inhibition by MOXI, which range from 0.93 to 398 μM and are dependent upon *in vitro* cell line and experimental conditions. Hence, the presumably "most bio-relevant" IC_{50} value of 29 μM for I_{Kr} inhibition by MOXI as per Alexandrou *et al.* (40) was chosen an input to the model and a corresponding sensitivity analysis conducted (see section 4 for further discussion).

#

Table 3. MOXI IC_{50} values for I_{Kr} current reported in literature

in vitro cell model	temp [ºC]	K^+ bath [mM]	holding potential [mV]	depolarization potential [mV]	repolarization potential [mV]	measurement potential [mV]	data source	IC_{50} [µM] (n)
HEK	22	4	-80	20	-80	-40	(40)	61 (0.96)
HEK	22	4	-80	20	-80	-80	(40)	65 (0.97)
HEK	22	4	-80	—	—	—	(40)	114 (0.94)
HEK	**35-37**	**4**	**-80**	**20**	**-80**	**-80**	**(40)**	**29 (1.14)**
AT-1	22-23	4	-40	20	-40	-40	(70)	0.93
CHO	22-24	5.4	-80	20	-40	-40	(71)	102.63 (1.1)
HEK	35-36	4	-80	0	-50	-50	(72)	>100
HEK	34-36	4	-80	20	-80	-80	(73)	35.7 (1)
HEK	—	—	—	—	—	—	(74)	122
CHO	room	5	-80	20	-40	-40	(75)	129
HEK	room	4	-80	40	-40	-40	(76)	86.2 (0.94)
HEK	36-38	4	-75	10	-40	-40	(77)	74.7
HEK	room	4	-80	60	-40	-40	(78)	99
CHO	21	3.2?	-70	40	-30	-30	(79)	80.5
HEK	36.5-37	5	-80	0	-50	-50	(80)	58.5 (0.92)
CHO	—	—	-70	40	-30	-30	(81)	398
CHO	room	4	-80	20	-50	-50	(48)	135.8 (0.91)
CHO	35-37	4	-80	20	-40	-40	(56)	34
HEK	—	—	—	—	—	—	(82)	102 (0.66)
CHO	24.5-25.5	4	-80	20	-40	-40	(83)	235

HEK – Human embryonic kidney cells; CHO – Chinese Hamster Ovary cells; AT-1 – Atrial tumor myocytes derived from transgenic mice; IC_{50} – Concentration of drug required to inhibition 50% of ion channel current; n – Hill coefficient; marked row indicates values used in simulations.

The inhibition factor was calculated using MOXI concentrations simulated by the PBPK model for the following bio-phases: (i) unbound plasma concentration; (ii) total plasma concentration; (iii) unbound heart tissue concentration; and (iv) total heart tissue concentration. Each bio-phase concentration was sampled at thirteen time points similar to those used in a typical Phase 1 study (i.e., 0, 0.25, 0.5, 1, 1.5, 2, 2.5, 3, 4, 6, 12, 18, 24 h post dose) and used as input to the CSS. The start of the treatment was assumed to be 09:00 clock time on day 1 and continues till 09:00 on day 2 (24 hours). The simulated QT interval was corrected for heart rate effect by Fridericia formula (18) and by placebo (QT interval simulated at same time of day with zero drug concentration) for each individual and each time point. Each of the result sets (corresponding to the four bio-phase concentrations) was then compared with clinically observed QT prolongation reported after single-dose administration of 400 mg orally.

3.4. Data to develop and verify the citalopram QSTS virtual twin model

The TT2006 ventricular cardiomyocyte cell model (34) was used to form a one-dimensional (1D) string mimicking the cross-section of the ventricular wall (as implemented within the CSS platform (29)) for simulating pseudoECG traces.

Four clinical reports containing measured plasma drug concentration and QT prolongation data (with CT doses ranging from 20 mg to > 1400 mg (>70-fold dose range) and the 100-fold range of maximum observed plasma CT concentrations) were chosen for the simulations (84-88). Electro-physiologically active primary metabolite desmethylcitalopram (DCT) and secondary metabolite didesmethylcitalopram (DDCT) were typically not measured along with parent plasma concentration in most clinical studies. The reported clinical settings, in terms of the number of subjects and their demographic and physiological parameters, were replicated as precisely as possible in the simulations. With the exception of the Ji *et al*. study (88), the metabolite concentrations were not typically reported. When not reported, the metabolite concentrations were estimated from the reported parent drug (CT) concentration using known parent/metabolite ratios calculated from the Ji *et al*. study (88) – 4 and 36 respectively for the CT/DCT and CT/DDCT ratios. Free plasma concentrations were estimated from plasma protein binding information obtained for the parent and its metabolites. The unbound plasma fraction (f_u) was estimated using the QSAR model implemented within the Simcyp Simulator V14.0 [Sheffield, UK] since experimentally measured values were not available for the metabolites (50, 89). The QSAR model for f_u in Simcyp is based upon the equations published by Lobell and Sivarajah (90), modified to explicitly account for a fraction of compound ionised at physiological pH considering pKa of the compound. The QSAR-based f_u of CT (0.23) was very similar to the reported value of approximately 0.2 (91). As CT, DCT and DDCT are very similar in chemical structure, the QSAR model was considered to reliably predict the CT metabolites (DCT and DDCT) f_u values. Therefore the predicted plasma protein binding for both metabolites DCT (f_u = 0.38) and DDCT (f_u = 0.52) was used in the absence of experimentally measured values. Although CT, DCT and DDCT may appear structurally very similar, the removal of methyl groups lead to significant difference in compound lipophilicity (LogP) and ionisation (pKa) which are structural properties used in the QSAR equation to predict f_u. Reduction in lipophilicity and increase in polarity of chemical lead to reduction in binding to plasma proteins resulting to increase in predicted value of f_u from CT to DCT to DDCT. The plasma concentrations of CT, DCT and DDCT for each of the four clinical scenarios are reported in Table 4.

Table 4. Plasma concentrations of CT, DCT and DDCT used during the simulations

Clinical Scenario	Clinical Study	Exposure ID*	Time Post Dose	Total Plasma Concentration (μM)			Free Plasma Concentration (μM)		
				CT (rep)	DCT (calc)	DDCT (calc)	CT (rep)	DCT (calc)	DDCT (calc)
CASE I	Unterecker 2012 (86)	S1E1	Day 2	3.795	0.949	0.105	0.873	0.361	0.055
		S1E2	Day 3	2.842	0.711	0.079	0.654	0.270	0.041
		S1E3	Day 4	2.454	0.613	0.068	0.564	0.233	0.035
		S1E4	Day 6	1.514	0.378	0.042	0.348	0.144	0.022
		S1E5	Day 23	0	0	0	0	0	0
CASE II	Tarabar 2008 (85)	S2E1	33h	1.470	0.368	0.041	0.338	0.140	0.021
CASE III	Liotier & Coudoré 2011 (84)	S3E1	7h^	18.126	4.532	0.504	4.169	1.722	0.262
		S3E2	21h^	7.460	1.865	0.207	1.716	0.709	0.108
		S3E3	45h^	7.398	1.850	0.206	1.702	0.703	0.107
CASE IV	Ji *et al* 2014 & FDA (88, 92)	S4E1	Day 1	0.195	0.051	0.005	0.045	0.019	0.002

** each set of drug and metabolite exposure points were simulated and given an ID for clarity in the discussion in the main text; rep. – reported in the respective clinical trial; calc. – calculated as described in the main text; CT – citalopram; DCT – desmethylcitalopram; DDCT – didesmethylcitalopram; ^ the time reported is post hospitalisation as the exact time of drug administration was not available in the study*

In vitro ion channel inhibition activity data for CT, DCT and DDCT for IKr, IKs and ICaL currents were extracted from the literature (Table 5). Drug concentration-dependent reduction of the maximal conductance of a particular ionic current was calculated directly in the CSS platform according to Equation 1.

The simple additive effect model (93) of all active moieties was assumed during simulations to calculate the total inhibition with the use of *in vitro* inhibition parameters of individual moieties provided in Table 5.

Five simulations were run with different settings to assess which scenario is most likely to explain the observed QT prolongation. Tested scenarios are as follows:

SIM 1 Free plasma concentrations of all moieties (CT, DCT and DDCT) and multiple ion channel inhibition information (I_{Kr}, I_{Ks} and I_{CaL}) for all moieties where I_{Ks} is the slow activating delayed rectifier potassium channel.

SIM 2 Total plasma concentrations of all moieties and multiple ion channel inhibition information for all moieties

SIM 3 Free plasma concentrations of all moieties but considering I_{Kr} inhibition only

SIM 4 Free plasma concentration of CT only to drive the response and using only I_{Kr} inhibition data for CT

SIM 5 Free plasma concentration of CT only to drive the response and using I_{Kr}, I_{Ks} and I_{CaL} inhibition data for CT

Table 5. Cardiac ion channel current inhibition data used in the simulations

Moiety	**IC_{50} in µM (Hill equation coefficient)**			
	I_{Kr}	**I_{Ks}**	**I_{CaL}**	**Reference**
CT	1.1 (0.83)	1059* (1)	60.28 (1)$	(94, 95)
DCT	2.1 (0.89)	3956* (1)	NA	(94)
DDCT	2.7 (0.92)	0.28 (0.88)	NA	(94)

**Calculated IC_{50} within the CSS platform based on %inhibition versus concentration profile reported in the reference; $ Hill coefficient was not reported in the study hence assumed to be 1; NA - the data was not available hence it was assumed negligible in all simulations; CT – citalopram; DCT – desmethylcitalopram; DDCT – didesmethylcitalopram; I_{Kr} , I_{Ks} , I_{CaL} represents rapidly activating delayed rectifier potassium channel current, slowly activating delayed rectifier potassium channel current, and late calcium channel current, respectively.*

The overdose clinical case reports (84-86) refer to the patients under intensive hospital care due to experiencing a life-threatening cardiac event after CT ingestion. Hence, many parameters were monitored such as heart rate, plasma K^+, Na^+ and Ca^{2+} ion concentrations in addition to the actual drug concentration. Further details of the simulated scenarios are provided below in a case-by-case format. The physiology parameter inputs used in the simulations for each of the four cases are described in Table 6.

Study-specific data used in the simulations are listed below.

CASE I: From the case report of a CT overdose of a 46 year old female subject (with the intention to commit suicide) published by Unterecker *et al*. (2012), drug exposure and clinical ECG data were obtained at multiple time points after drug ingestion (86). The demography (age and gender) and physiology (heart rate, plasma K^+, Na^+, Ca^{2+} ion concentrations) reported in the clinical case study were simulated using the reported CT plasma drug concentrations and estimated metabolite concentrations. In other words, a 'virtual twin' of the actual subject was

built *in silico* and used to assess the observed QT prolongation. Many parameters defining the subject physiology were measured; however, there were some (e.g. heart wall thickness, conductance, etc.) which were not available, so those unavailable parameters were calculated using the covariate models of a healthy Caucasian population physiology from age and gender of a patient (96). The values of the heart rate and plasma ion concentrations reported in the clinical studies were either the average values recorded over a period of a few seconds or minutes or were a specific value at the time of measurement, both of which are known to have inter-occasion variability. To account for such uncertainty, each drug concentration effect was simulated, for an individual subject, 5 times considering known 'within-subject variability' in those parameters implemented within the CSS platform.

CASE II: Tarabar *et al*. (2008) reported the case of a 36 year old woman who ingested 50 tablets of 20 mg CT (approximately 1000 mg dose) with wine (85). The clinically measured drug concentrations, estimated metabolite concentrations and physiological parameters (such as heart rate and plasma ion concentrations) were used as inputs to the model. Each concentration time point was simulated 5 times. The model doesn't take into account the influence of alcohol on the heart rate mechanistically; however, the measured heart rate values were used as input data which implicitly considers the effect of alcohol on the heart rate in our simulations.

CASE III: In the Liotier & Coudoré 2011 study, a 54-year old female subject ingested an unknown number of CT tablets that demonstrated a 100-fold higher plasma drug concentration as compared to the typical plasma drug concentrations reported with a therapeutic dose level (20 mg) (84). She also suffered from hypokalemia. All known clinical parameters (age, gender, plasma K+, Na+, Ca2+ ion concentrations, heart rate, etc.) were included in our simulations to mimic the clinical scenario as precisely as possible. Each concentration time point was simulated 5 times to factor in uncertainty or inherent variability in those physiological parameters as described earlier.

CASE IV: QT prolongation information for a 20 mg CT dose was obtained from the US FDA assessment report (87) which, to the best of our knowledge, is not published in the peer-reviewed journals. The plasma concentrations of CT, DCT or DDCT were not reported in the FDA assessment report. Hence, the plasma drug concentrations reported in another informative

clinical study conducted with a 20 mg CT dose was used to simulate the effect at a 20 mg dose level (88) where CT, DCT and DDCT concentrations were reported.

Table 6. Physiology (systems) parameters used in the simulation cases I-IV

Physiology Input Parameters	CASE I Simulated (Clinical)	CASE II Simulated (Clinical)	CASE III Simulated (Clinical)	CASE IV Simulated (Clinical)	Reference
Gender	Female (Female)	Female (Female)	Female (Female)	9 Females; 9 Male (NR)	As Reported/Assumed
Age (years)	46 (46)	36 (36)	54 (54)	27±7 (NR)	As Reported/Assumed
Cardiomyocyte Area (μm^2)	4342±1360 (NR)	2936±919 (NR)	5963±1882 (NR)	2096±806 (NR)	Calculated with known covariate model from age and gender (36)
Left Ventricular Wall Thickness (cm)	1.45 (NR)	1.36 (NR)	1.54 (NR)	1.28±0.13 (NR)	Calculated with known covariate model from age (36)
Cell Capacitance (pF)	115±36 (NR)	78±24 (NR)	158±50 (NR)	56±21 (NR)	Calculated with known covariate model from age and gender (35)
Heart Rate	As reported	As reported	As reported	Calculated (NR)	Reported or calculated if not reported, with known covariate model from age, gender and time of day (32)
Plasma K^+ [mM]	4.05±0.4 (normal)	3.1±0.3 (3.1)	2.9±0.3 (2.9)	4.15±0.8 (NR)	Calculated from covariate model with age, gender and time of day (97)
Plasma Na^+ [mM]	135±1.9 (normal)	134±2 (133)	135±1.9 (NR)	140±4 (NR)	
Plasma Ca^{++} [mM]	2.2±0.1 (normal)	2.25±0.1 (2.3)	2.2±0.1 (NR)	2.4±0.3 (NR)	

NR - Not Reported in the clinical study report

Moreover, the FDA letter only reported ΔQTc (QT prolongation by the drug in comparison to placebo) and the correction method for heart rate was not clearly specified. Hence, ΔQTc was

calculated from our simulation results (QT prolongation triggered by the drug in comparison to QT at zero drug concentration under the same physiological conditions) using the Fridericia correction method (QTcF). As clinical data for CASE IV is a population mean value rather than the response of particular patient, 16 virtual healthy Caucasian individuals (50% females) were simulated based on default covariate models implemented in the CSS platform and compared the population mean values of ΔQTcF generated from the simulated trial to the observed clinical trial. CT is known to modify the electrophysiology of the heart via the CNS, an effect that could contribute to the observed QT prolongation. The impact of the CNS-mediated cardiac effect of CT was not explicitly modelled in this current work. However, the clinically measured heart rate values were used at different drug concentration-time points implicitly considering the effect of CT on the heart rate via the CNS modulation. The simulated QT prolongation observed with the above described four cases (CASE I-IV) was then compared with the clinically measured QT prolongation.

4. Results and Discussion

4.1. Incorporation of circadian variability in HR

A circadian rhythm is a biological process that displays an endogenous, entrainable oscillation of roughly 24 hours (98). In humans there are multiple physiological processes which follow the circadian clock, including the heart rate (HR) (99). In our study context, however, the circadian rhythm of the heart rate is one of the most important, since it may both influence the QT length and interfere with the drug effect (100). The mathematical and statistical modelling of the circadian variation of the heart rate has been previously studied. Nakagawa and colleagues reported results of a study which involved 44 (but 20 were included into the analysis phase) healthy individuals. Subjects showed a significant circadian heart rate rhythm and based on the collected data the authors proposed a cosinor model to describe such phenomenon, although they did not differentiate between male and females which limits the practical use of the derived model (101). Similar models, carrying identical limitations were proposed independently by Massin and colleagues and Li and colleagues (102, 103). 57 healthy children and 115 healthy, non-smoking adults were included respectively and the 24-hours ECG measurements were used to derive the regression models. Probably the most detailed analysis of the heart rate variation was presented by Bonnemeier *et al*. (104). A large group of 166 healthy individuals (81 females, 85 males) characterized by a wide age range (20–70 years) was studied. The authors analysed differences of heart rate circadian profiles for hourly aggregated measurements in a groups stratified by age decades, separately for female and male subjects. The authors did not, however, model their data. There is also a large number of publications where circadian heart rate variation is discussed among various subpopulations (athletes, truck drivers, welders) and diseases (myotonic dystrophy, angor patients) (105-108). Although to my best knowledge none of them proposed a model flexible enough and described in enough detail to be directly applicable for the generation of a virtual human population where heart rate is an attribute specific for every individual, and this was the main reason it was decided to develop a new model.

The preliminary model included dummy variables for each Hour, dummy variable for Sex, quadratic effect of Age and all pairwise interactions. Many terms in this preliminary model were found not significant, as indicated by the robust t-tests for model coefficients. The robust t-test takes into account the dependence between observations coming from the same subject. Non-significant terms (p-value>0.05) were dropped from the model sequentially one by one.

Additionally it was found that the Hour variable may be modelled more parsimoniously by a linear combination of sine and cosine functions. The final model received the following form:

$$\log(RR) = \beta_0 + \beta_1 Sex + \beta_2 Age + \beta_3 Age^2 + \beta_4 \sin\left(\frac{2\pi}{24} Hour\right) + \beta_5 \cos\left(\frac{2\pi}{24} Hour\right) + \beta_6 \sin\left(\frac{2\pi}{24} Hour\right) \times Sex + \beta_7 \cos\left(\frac{2\pi}{24} Hour\right) \times Sex + \varepsilon, \quad \varepsilon \sim N(0, \sigma), \tag{2}$$

where

β – regression coefficient;

ε – normally distributed error term;

σ – standard deviation of error term;

Sex – 1 for males and 0 for females;

Age – age in years;

Hour – value from 0 - 24 range

The model parameters were estimated using the maximum likelihood method in the R system for statistical computing and are given in below in equation 3.

$$\begin{aligned} \log(\hat{RR}) &= 7.163 + 0.0961\ Sex - 0.0243\ Age + 0.00027\ Age^2 \\ &\quad + 0.1055 \sin\left(\frac{2\pi}{24} Hour\right) + 0.0664 \cos\left(\frac{2\pi}{24} Hour\right) \\ &\quad - 0.0155 \sin\left(\frac{2\pi}{24} Hour\right) \times Sex + 0.0608 \cos\left(\frac{2\pi}{24} Hour\right) \times Sex, \sigma \\ &= 0.15 \end{aligned} \tag{3}$$

All coefficients were statistically significant. Figure 3 shows the graphical representation of the model. The visual predictive checks showed an overall good fit of the model to the data. The dispersion of residuals did not exhibit dependence upon any of the explanatory variables. The coefficient of determination R^2 = 0.39, i.e. 39% of the variation observed in log(RR) can be explained by the estimated regression equation.

For the PhysioNet data set RMSE (Root Mean Squared Error) = 128 ms and MAPE (Mean Absolute Percentage Error) = 12.3%. In the case of the validation data set RMSE = 165 ms and MAPE = 17.1%. It is a well-known fact that estimators derived by the method of maximum likelihood have many desirable properties, on the other hand ML estimators are sensitive to the presence of outliers in the data. In order to check the stability of estimates the regression parameters were additionally estimated using a wide range of, so called, robust regression estimators. Parameter estimates were virtually unchanged from the maximum likelihood ones. It was found that only a large value of P (P = 180) was able to account for the long memory observed in the data and gives a satisfactory fit. The estimate of the standard deviation of error term was 0.096.

Figure 3. Graphical representation of the RR model for females (A) and males (B) respectively, left inner axis is age.

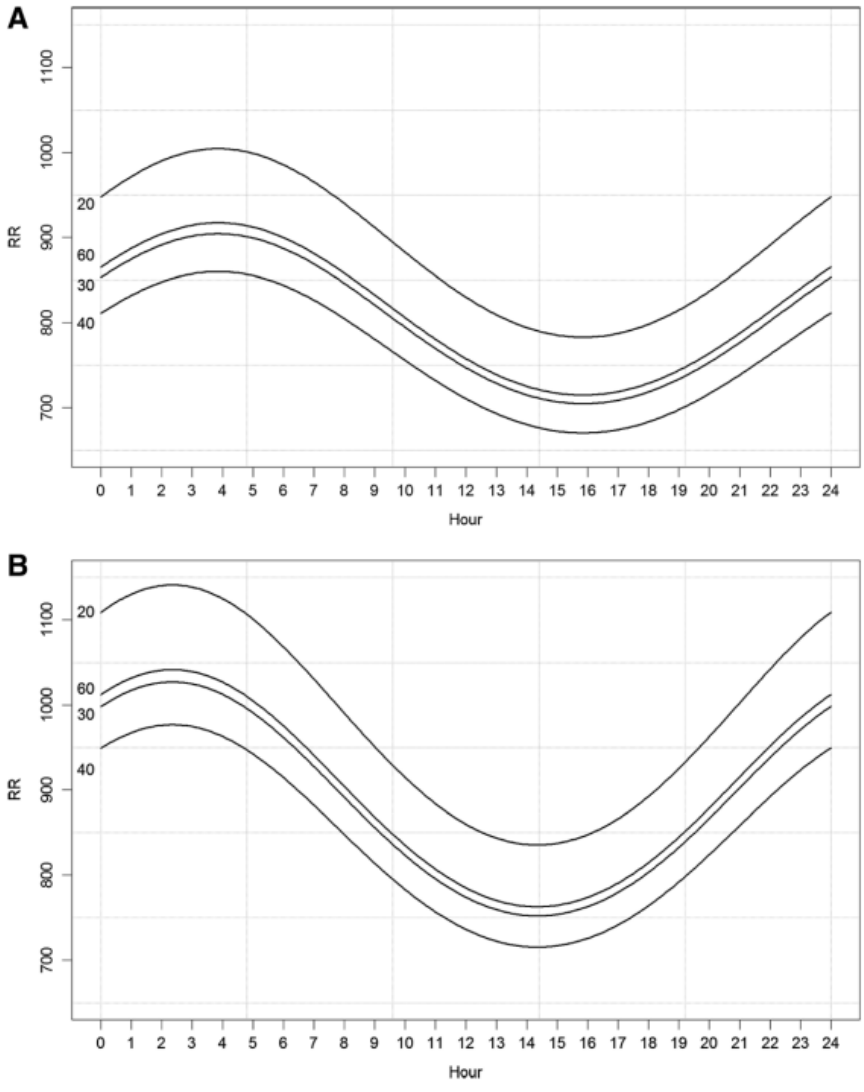

QT response at a MOXI concentration of 3.8 μM at different times of the day was simulated using the ToxComp platform. When single point baseline correction was applied, the ΔQTcF obtained at different times of the day at a MOXI concentration of 3.8 μM is shown in Figure 3. Generally, during TQT studies an oral dose of MOXI 400 mg is given in the morning, hence Cmax is obtained between morning and noon i.e. between 8.00 to 12.00. At 8.00 and 12.00, the simulated ΔQTcF were respectively 10.75 ms and 15.87 ms, which is consistent with the clinically observed ΔQTcF of 10–15 ms (109). When an individualized baseline with circadian correction was applied, ΔQTcFi of 5–6 ms was obtained at all times of day which is also consistent with the clinically observed ΔQTcFi of 6–7 ms (33). The obtained results indicate that the implemented heart rate circadian rhythm model within the CSS platform is able to simulate the circadian variability of a model drug. Comparison with the published clinical trial results for the model drug suggest that the CSS system, with the built-in heart rate model, is able to realistically represent cardiac electrophysiological drug effect with its variability, regardless of the correction method. However, as there are a large number of parameters describing the physiological variability in the virtual population generator module, it is hard to precisely assess the net influence of the heart rate on the system output, and a separate study will be run for such a purpose. Although results of the simulations run without the use of a heart rate model, i.e. with the use of a constant value of HR during the day, suggested that an important component is missing. With the implementation of circadian heart rate generator, the CSS platform would allow more accurate simulation clinical ECG profiles and would help achieve further goals of this thesis that is to assess and establish the utility of CSS platform in addressing research questions from early discovery to late stage clinical development.

4.2. Application of QSTS approach during Phase I or thorough QT trial design

As described in the introduction, the risk of TdP has been ascribed for drugs spanning wider therapeutic areas, other than cardiovascular drugs; hence, it has become important to assess the TdP risk for any new medicine. Thus a TQT trial that is a dedicated and well-controlled clinical trial to quantify the propensity of drug to prolong QT/QTc at therapeutic and supra-therapeutic dose levels as compared to positive control have become an essential study to establish TdP risk of any new medicine under development. Due to inherent physiological variability and the need to detect very small statistical change in QT interval prolongation, estimating the power of the study that is able to reach the concluding endpoint in TQT trial is of paramount importance as cost of failure to obtain statistical power to reach the conclusive endpoint could be very high.

The multi-scale QSTS models such as CSS platform can bridge the translational gap in cardiac safety assessment with the use of *in vitro* dynamic ion channel inhibition data and expected exposure levels to simulate subsequent effects on ECG profile in virtual patients, which represent an array of physiologies expected in clinical practice (22, 29). Such QSTS approach thus allows simulations of TQT trials. Such simulated TQT trials could allow studying various study designs, identify the sources of variability and in general ask various "what if" questions before conducing the clinical study. Such simulations could help reduce, refine or avoid the need of clinical trials. Such ability was demonstrated via two TQT trial examples of TOL and FESO.

4.2.1 Tolterodine TQT trial simulations

The clinically observed ΔΔQTcF (ms) at 2 mg and 4 mg bid dose levels for population of 48 subjects was reported in study by Malhotra *et al*. (41). Sweeney *et al*. (110) have analysed the TQT trial clinical data using population PKPD model to estimate the population mean of EM and PM groups. The simulated QT prolongation data of 48 subjects, separated by EM (N=27) and PM (N=21) groups are reported along with clinical ΔΔQTcF data for 2 mg and 4 mg dose groups in Figure 4A and 4B, respectively. The simulations were run using four concentration levels to study the most bio-relevant exposure surrogate to explain the observed ΔΔQTcF data – (i) total plasma concentration; (ii) unbound plasma concentration; (iii) total heart tissue concentration, and (iv) unbound heart tissue concentration. The results clearly showed that the total heart tissue and total plasma concentrations over-estimated the ΔΔQTcF. There was no significant difference between the predictions using the unbound plasma and unbound heart tissue concentrations mainly because the estimated partition coefficient for TOL between heart tissue and plasma is approximately 0.45 and the fu_{Heart} of 0.066 thus unbound heart tissue and plasma exposures were similar. The predictions using the unbound plasma and unbound heart tissue exposure levels were closest to clinically observed ΔΔQTcF for both EM and PM groups and at both dose levels (Figure 4).

Figure 4. Observed and simulated ΔΔQTcF (ms) for a 2-mg BID and b 4-mg BID doses.

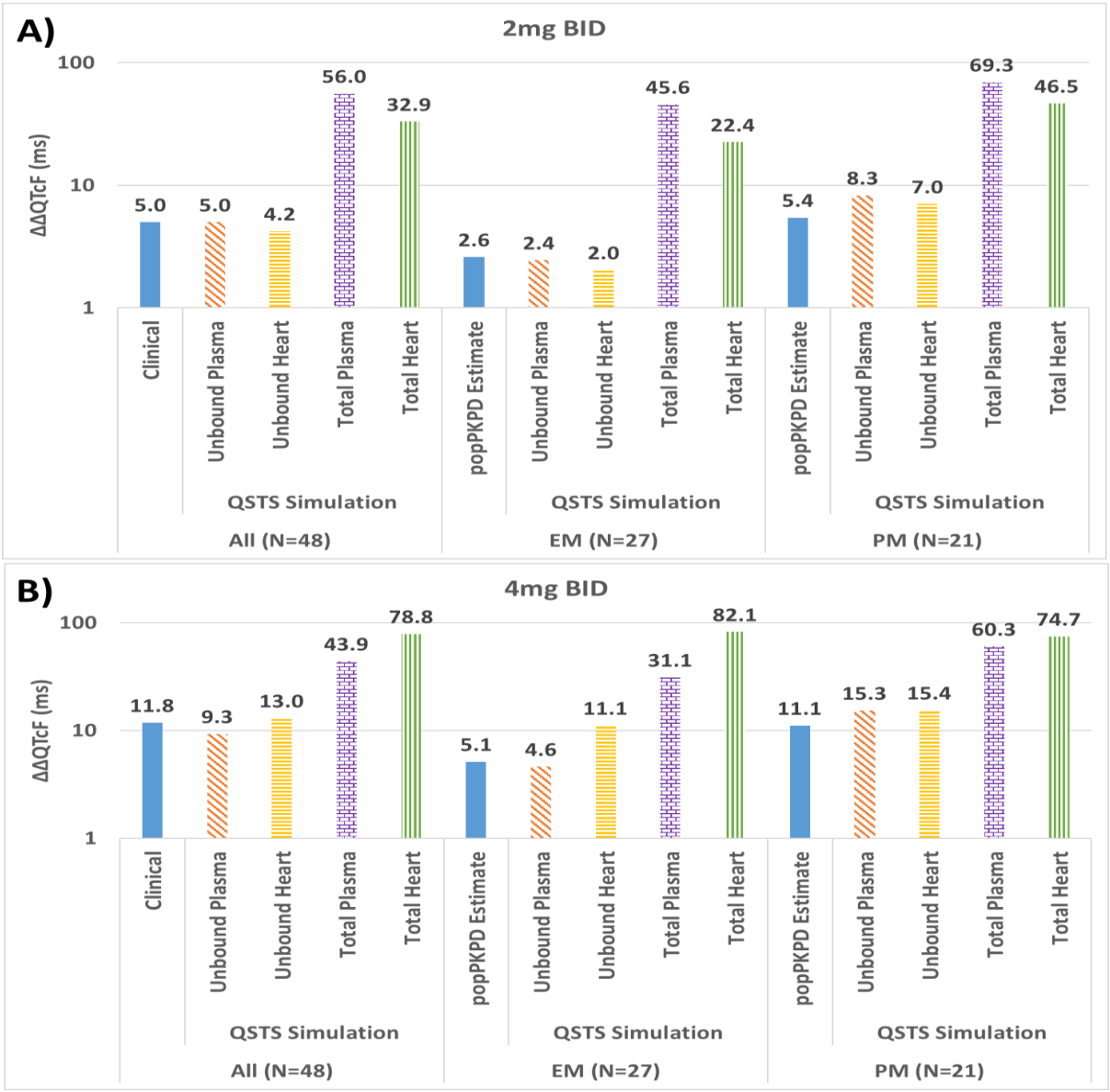

Blue solid bars represent observed data, orange diagonal striped bars represent the simulated data with unbound plasma concentration as operating concentration, yellow horizontal striped bars represent simulated data with unbound heart tissue concentration as operating concentration, purple brick patterned bars represent the simulated data with total plasma concentration as operating concentration, green vertical striped bars represent simulated data with total heart tissue concentration as operating concentration. Observed data for extensive and poor metabolizer groups was obtained by population pharmacokinetic-pharmacodynamic (popPKPD) modelling of clinical data. The black thin error bars represent the 95% confidence interval around the mean value.

Figure 5. Clinically observed and simulated ΔΔQTcF (ms) at therapeutic and supra-therapeutic dose levels of TOL along with positive control drug MOXI for thorough QT trial of TOL

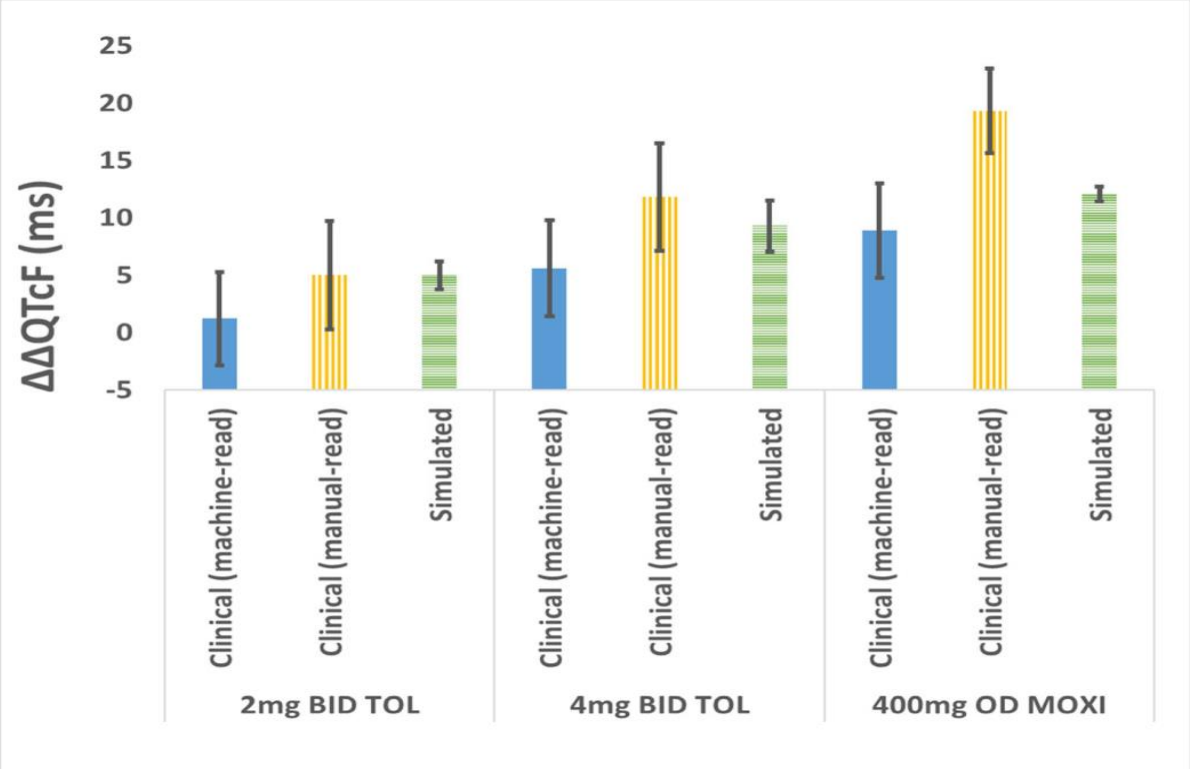

Clinical ΔΔQTcF calculated from machine-read electrocardiogram is represented with solid blue bar, clinical ΔΔQTcF calculated from manual-read electrocardiogram is represented with vertically striped yellow bar, and simulated ΔΔQTcF is represented with horizontally striped green bar. The black thin error bars represent the 95% confidence interval around the mean value.

Figure 5 shows the comparative ΔΔQTcF prolongation from simulated and clinical TQT trial results for therapeutic and supra-therapeutic dose levels of TOL along with positive control MOXI. The vertical error bar indicates the 95% confidence interval around the mean ΔΔQTcF from the clinical study and simulated population.

The concentration-ΔΔQTcF relationships for both dose levels and by EM and PM groups are provided in Figure 6. Figures 6A and 6B show the relationship for 2 mg and 4 mg BID dose levels while the Figures 6C and 6D show the relationship for EM and PM groups, respectively. There is no considerable difference in slopes of concentration-ΔΔQTcF relationship, which ranged from 10-15 ms/ng/mL.

Figure 6. The concentration-ΔΔQTcF relationships for TOL and metabolite 5-HMT

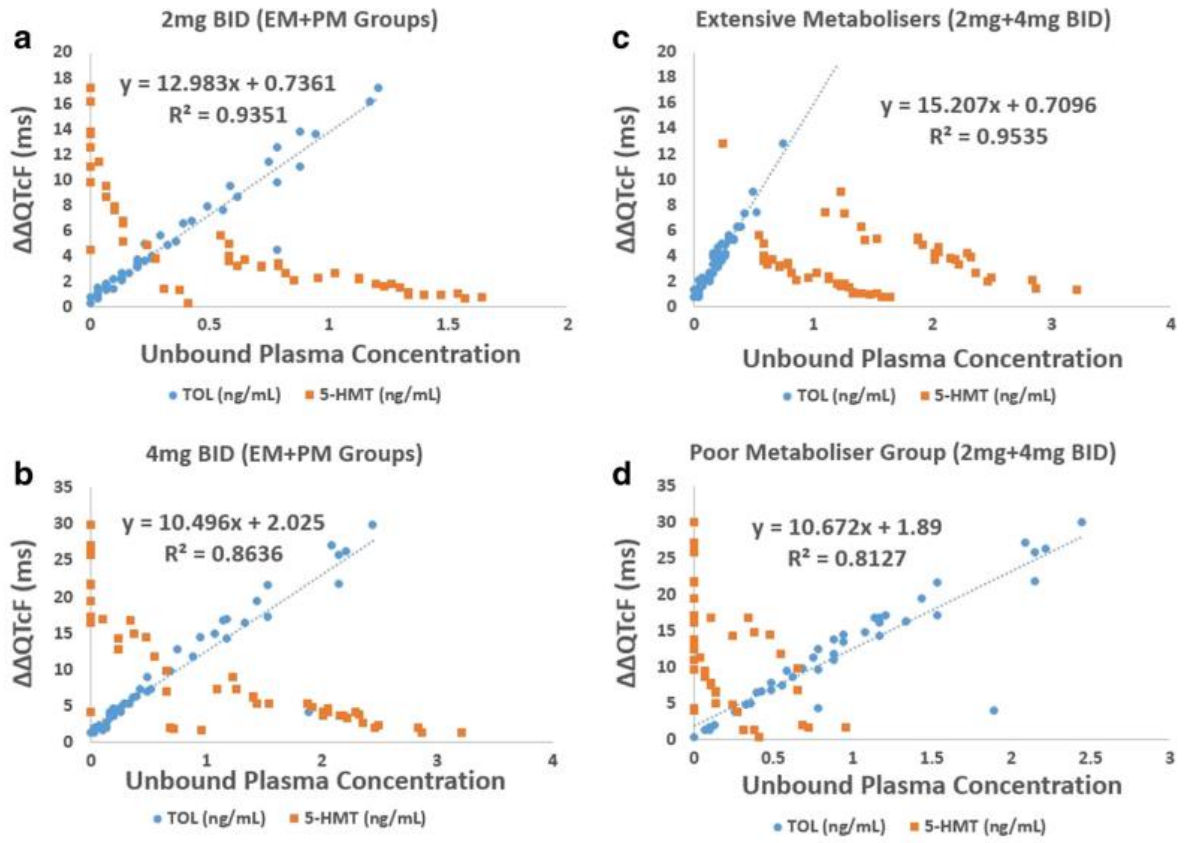

The concentration-ΔΔQTcF relationships for TOL and metabolite 5-HMT after administration of 2-mg BID dose (a) and 4-mg BID dose (b) of TOL and for extensive metabolizer population group (c) and poor metabolizer population groups (d).

Figure 6 clearly shows poor relationship between 5-HMT concentration and ΔΔQTcF indicating that the metabolite 5-HMT had negligible contribution to the predicted QT prolongation while the TOL concentration was linearly and positively correlated with the ΔΔQTcF. EM subjects showed larger values of slope than the PM subjects (approx. 5 ms/ng/mL larger) while the lower dose had slightly higher slope than the higher dose level.

4.2.2. Fesoterodine TQT trial simulations

The clinically observed ΔΔQTcF (ms) at 4 mg and 28 mg FESO dose levels were reported in study by Malhotra *et al.* (45). Figure 7 shows comparative values of ΔΔQTcF (ms) from simulated trial and observed data on day 3 at both dose levels.

Figure 7. Clinically observed and simulated ΔΔQTcF (ms) at therapeutic (4 mg) and supratherapeutic dose (28 mg) levels of FESO in thorough QT trial.

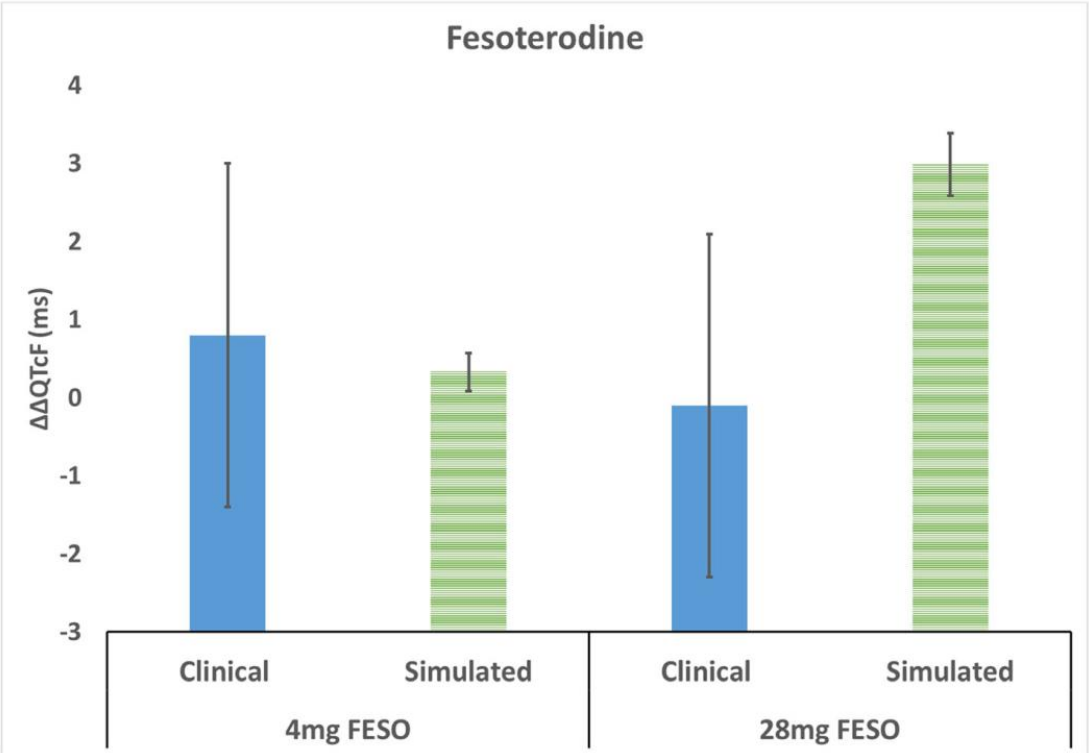

Clinically observed ΔΔQTcF is represented with solid blue bar and simulated ΔΔQTcF is represented with horizontally striped green bar. The black thin error bars represent the 95% confidence interval around the mean value.

The model predicted the QT interval prolongation really well at lower dose level of 4 mg; however, the clinical results showed no change or slight shortening of QTcF interval (-0.1 ms) at higher dose of 28 mg while the model predicted small QT prolongation (3 ms). The simulated variability was much smaller than that observed in the clinical trial and the simulated results are within the 95% confidence interval reported in the clinical study (also showed as vertical error bars in Figure 7. Thus the results based only on *in vitro* cardiac safety input data is in good agreement with clinical TQT trial.

TOL, an antimuscarinic agent used for the treatment of overactive bladder, has an equipotent metabolite 5-HMT. TOL is found to be a potent inhibitor of hERG channel while the metabolite 5-HMT is a magnitude less potent in inhibiting hERG. Both TOL and 5-HMT inhibit late calcium channel although with very low potency. The unbound fraction of TOL and 5-HMT in plasma is around 3.7% and 36%, respectively (41). Therefore, even though the exposure levels

of TOL is many-fold higher in CYP2D6 PM subjects, the effective free plasma exposure of net therapeutically active moieties are comparable in EM and PM groups negating the need for dose adjustment for PM group. However, the cardiac safety profile could be different due to significant difference in potency of TOL and 5-HMT in inhibiting the hERG channel. As the TOL is >10-fold more potent hERG inhibitor than 5-HMT, a considerably higher the QT prolongation is expected in PM subject group. However, simulated results as well as clinical observations indicate only a small increase in QT prolongation in PM subjects as compared to EM subjects mainly due to much higher binding of TOL to plasma proteins moderating the increase in total plasma concentration in PM subjects. Natural frequency of CYP2D6 PM polymorphism in normal population is around 8%, however, the clinical study, and hence the simulated trial, was enriched with higher proportion of PM (45%) subjects to sufficiently represent the high risk PM group subjects. The simulation results indicated the QSTS model accurately predicted the clinical QT prolongation not only for therapeutic and supra-therapeutic dose levels but also was able to differentiate the effect EM and PM exposure levels on QT prolongation. It is also important to note that the clinically observed QT interval prolongation estimated with machine-read ECG is systematically lower than the manual read ECG (Figure 5). When the QSTS model is assessed in terms of its predictive performance for such smaller values of QT interval prolongation, it becomes important to understand the variability and uncertainty associated with the clinical data and/or the measurement technique. There were considerable differences in QT prolongation from clinical study noted between manually read and machine ECG, hence both machine-read and manual-read values were provided along with predicted results (Figure 5). For MOXI arm, the simulated results were within the reported 90% confidence interval of clinical data from machine read ECG while higher than the reported value with manually read ECG (18). There exists inter-study variability in QT interval prolongation after 400 mg MOXI once-daily (OD) treatment due to multiple of study design factors such as encapsulation of tablet for purpose of blinding and manufacturer of the formulation, etc. (6). It was shown there that the prediction for MOXI were reasonably good at much wider pooled clinical data set from six independent studies thus here the prediction for MOXI positive arm was considered acceptable. For TOL 2 mg BID as well as 4 mg BID the simulated results were well within 95% confidence interval of clinically reported values from both machine-read and manual-read ECG results. There are no animal or human studies reporting the heart tissue exposure of TOL or 5-HMT hence the simulated heart tissue exposure cannot be fully verified. The issues and uncertainties around the bio-relevant exposure levels driving the cardiac response and limited knowledge in public literature have been discussed

elsewhere (23, 26). The impact of model selection on MOXI, for example O'Hara Rudy 2011 model (69) tends to predict larger QT prolongation than the ten Tusscher 2006 model (34) for the same input parameters (23) was studied previously, however a well-defined systematic studies are needed to analyse such model comparison at single cell level (action potential duration) as well as ventricular wall level (QT prolongation) simulations to provide further recommendations. More experimental data at both *in vitro* and *in vivo* level and collaborative research initiatives are required to complement QSTS modelling results to test or establish hypotheses and move the field of cardiac risk assessment forward.

Another important measure to assess the predictive performance of the QSTS model would be to compare its ability to simulate the effect (ΔΔQTcF) versus exposure (drug concentration) profile. The slope of simulated ΔΔQTcF-concentration relationship (10-15 ms/ng/mL) were very similar to the reported from clinical data analysis (population mean point estimate of 13.4 ms/ng/mL) for unbound plasma concentration. Moreover, the QSTS model showed no considerable difference in EM and PM groups similar to the observation made from clinical data analysis by Sweeney *et al*. (110). The contribution of metabolite 5-HMT in QT prolongation was negligible as evident from no correlation between 5-HMT concentration and QT prolongation at both dose levels and for both EM and PM groups. This observation from the simulated results can also be verified with another TQT study report for FESO, the ester pro-drug of 5-HMT. Clinical TQT trial of FESO with 4 mg and 28 mg dose resulted in negligible QT prolongation or slightly shorter QT prolongation as compared to placebo. The simulations predicted similarly low to negligible QT prolongation at both dose levels of FESO. This clearly establishes the outcome of simulation results from TOL simulation that the 5-HMT does not prolong QT interval even though it inhibits hERG channel. Ability to inhibit the calcium channel could explain the slight shortening of the QT interval in clinical TQT trial especially at higher dose level (28 mg FESO) because the potency of 5-HMT to inhibit the calcium channel is very low (Table I) thus measurable inhibition of calcium current can only be achieved at higher exposure levels. Simulations, although recovered the observed QT prolongation range of both dose levels really well, could not mimic the QT shortening trend with dose. Although not statistically significant, the clinical data showed slightly lower QT prolongation at higher dose of FESO than at lower dose. This could be due to fact that the IC50 value for calcium channel inhibition was not available as the maximum concentrations studied *in vitro* lead to around 17% inhibition of calcium current thus making it difficult to derive accurate IC50 value. More accurate IC_{50} value for calcium channel inhibition may allow the

QSTS model to recover the QT shortening effect at higher exposure levels. The potency of TOL and 5-HMT is similar in inhibiting the calcium current based on limited data available from literature (48, 49). As observed with lower slope of ΔΔQTcF-concentration profile at higher dose (4 mg) compared to the slope at lower dose (2 mg) in Figure 6, the QSTS model was able to estimate the trend of reduction in QT prolongation effect at higher dose levels based on limited input data for calcium channel inhibition. Thus, the success of the QSTS model to predict the clinical QT interval modification by drug strongly depends on quality and accuracy of input data to the IVIVE methodology.

It was shown previously that the metabolites of CT were very important in predicting the QT prolongation profile of CT (26) however, here the metabolite 5-HMT did not contribute to QT prolongation after TOL treatment even though 5-HMT was moderate hERG channel blocker. Thus, QSTS approaches also allow testing of various hypotheses such as the impact of metabolite on safety and tolerability of the drug treatment. QSTS models can be applied at early discovery levels as the models can be fed with chemical structure to predict the QT prolongation with use of QSAR techniques. As the drug progresses in the development, the model can be enriched with better quality input data, and the virtual TQT trials can be simulated when sufficient knowledge on the PK of drug and metabolites becomes available along with *in vitro* cardiac safety assessment profiles, as it was presented in the current study. Once sufficiently verified such QSTS models can also be used to refine and optimize the clinical study designs.

With examples of TOL and FESO, the utility of the QSTS approaches to bridge the translational gap in cardiac safety assessment and simulate virtual TQT trials was established. Such simulations could complement and reduce the clinical studies or help optimise clinical trial designs. Such QSTS approaches can also help build and test hypothesis such as assessing the role of unbound versus total plasma concentration or assessing the contribution of electro-physiologically active metabolite and allow understanding impact of population variability such as genetic polymorphism on the cardiac safety profile of drugs. Population based QSTS models could also help address late stage development questions such as understanding the impact of metabolic drug-drug interactions on cardiac safety risk and identify the high-risk clinical situations for potential TdP. Adoption of such QSTS modelling strategies from early stages of drug discovery and development and enrichment of model and information along with drug product life cycle could allow bridging translational gap in clinical cardiac safety assessment.

4.3. Application of QSTS approach during late drug development (Phase III):

As described in the introduction, QSTS based progressive cardiac risk assessment strategy was proposed as part of this thesis, where the risk assessment for a novel compound is refined progressively as clinical knowledge is enriched through predict-learn-confirm cycles. The individual model components are iteratively verified/refined, to reduce uncertainty and increase confidence, making them adaptable to more adequately address questions around therapeutic performance, as they arise during clinical development. The Cardiac Risk Algorithm as proposed by Polak *et al*. (28) is one component model that can be particularly informative during early phase development to estimate potential cardiac safety risk even in the absence of detailed information about human PK and PD, as sensitivity analyses may be performed to simulate a range of possible clinical scenarios. As more PK and PD information about the drug becomes available with further drug development, these initial predictions can be verified and refined, and ultimately may be superseded by a more detailed PBPK-QSTS model platform. Once sufficiently verified, the established and enriched model can be used to simulate clinical scenarios to evaluate effects of intrinsic and extrinsic factors (i.e., special populations, drug-drug interactions, co-morbidities) to establish the clinical cardiac risk scenarios [Figure 1].

To illustrate this approach a series of simulations were performed to reflect virtual administration of the anti-infective, moxifloxacin (MOXI). MOXI was chosen as an exemplar compound as it is the most commonly used positive control in TQT trials and thus has well established human PK and PK-ECG profiles. Furthermore, MOXI is active against *Mycobacterium tuberculosis (Mtb),* the causative pathogen of tuberculosis (TB), and thus is administered as a component of anti-TB drug regimens. Cardiac risk assessment in TB is of specific importance, as many existing and emerging anti-TB agents have a known or suspected propensity for QT prolongation. As the application of a model-based QST strategy for progressive cardiac risk assessment could be advantageous in the prioritization of compounds for inclusion in anti-TB regimens, MOXI serves as an illustrative example of how this approach could be applied during preclinical and early clinical development. Here we report a utilization of the cardiac QST models implemented within Cardiac Safety Simulator (CSS) platform (Certara, Sheffield, UK), previously known as ToxComp platform (30) for the quantitative prediction of QT prolongation in humans at therapeutic dose and the risk of causing TdP. The impact of potential supra-therapeutic concentration of MOXI was assessed in causing TdP *in*

silico as well as existing conditions such as hypokalemia which were not part of early stage risk stratification algorithm.

The simulated plasma concentration-time profile obtained after 400 mg MOXI oral dose in fasted state overlaid with clinically observed data is reported in Figure 8a. The comparative average unbound plasma, total plasma, unbound heart tissue and total heart tissue concentrations are shown in Figure 8b. The concentrations in heart tissue are almost 4-fold higher than the corresponding plasma concentrations and there is a slight delay in achieving T_{max} in heart tissue (2.6 h) as compared to plasma (2.4 h) due to time taken to perfuse and partition in the heart tissue from systemic circulation.

Figure 8. Simcyp simulated total plasma concentration time profile after 400mg MOXI oral dose under fasted condition

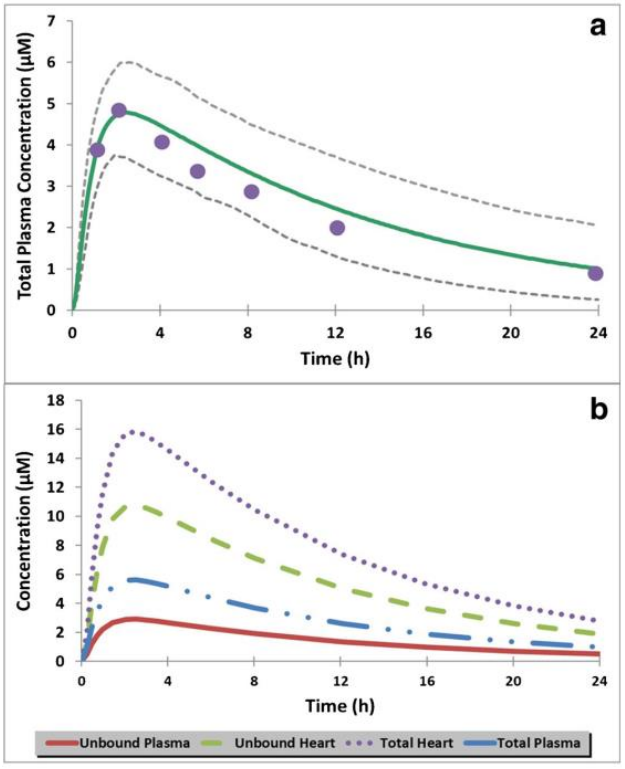

Simcyp simulated total plasma concentration time profile (thick green line is arithmetic mean, dotted gray lines are 5th and 95th percentile) from 20 virtual subjects overlaid with mean profile (filled blue circle markers) obtained from clinical study by Stass et al. (21) after 400-mg oral dose of MOXI in fasted state; b Simulated population mean of unbound plasma, total plasma, unbound heart tissue, and total heart tissue concentrations of MOXI.

Considerable variability in clinical studies measuring QT prolongation is reported in literature mainly due to the differences in study protocols, baseline and heart rate correction approaches, demographic differences and drug formulations. For example, over-encapsulation of MOXI (and the investigational product) is sometimes used for blinding purposes in TQT trials, which may contribute to inter-study variability in MOXI pharmacokinetics, specifically mean transit time and time of peak plasma MOXI concentration as shown by Florian *et al* (111). Due to this and other such variations in clinical trial design, before embarking on QSTS model verification the reported QT prolongation from clinical study reports were summarized where placebo baseline and heart rate corrected QT prolongation, known as ΔΔQTc, was reported. Six clinical study reports (112-117) were identified that provide the ΔΔQTc profiles post-MOXI 400mg oral dose where matching PK and ΔΔQTc–time profiles were reported; these are depicted in Figure 9 along with a pooled average. The profiles were digitized from the graphs reported in study reports using GetData Graph Digitizer software version 2.26.

Figure 9. Variability in clinical *ΔΔ*QTc after 400-mg MOXI oral dose

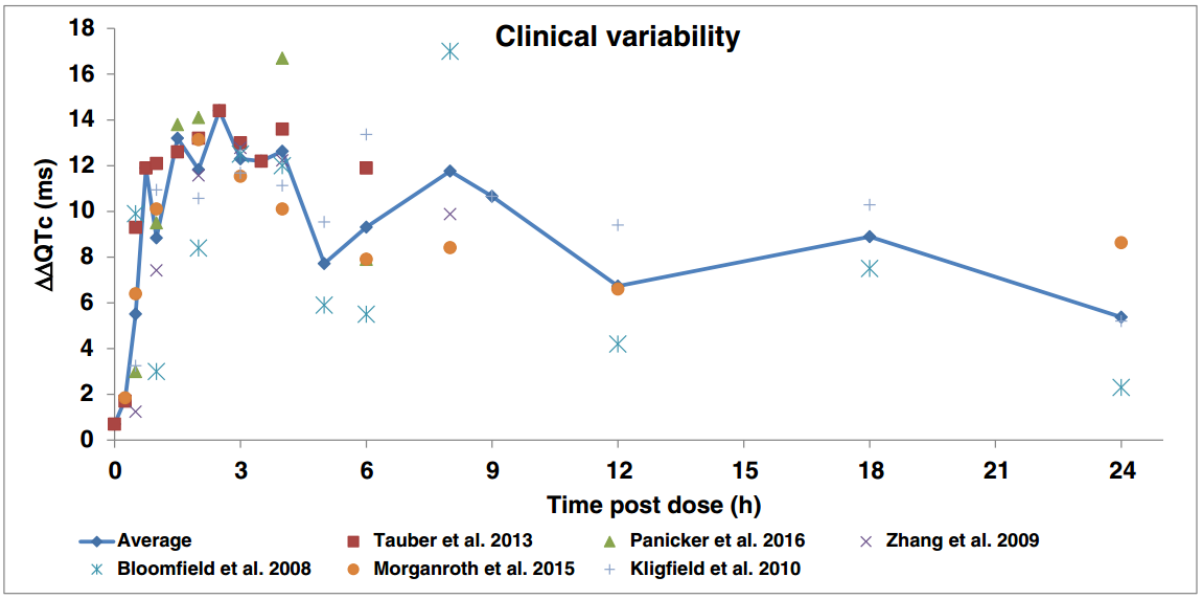

The simulated ΔΔQTcF prolongation derived using simulated MOXI concentrations in the four bio-phases are shown in Figure 10 and are overlaid with the pooled average ΔΔQTc as shown in the Figure 9. Figure 10a shows the results when unbound plasma MOXI concentration was used as the operating concentration to drive the cardiac QST model, with Figures 10b, 10c and 10d showing the equivalent for total plasma, unbound heart tissue, and total heart tissue MOXI concentrations, respectively. Comparison of the simulated and observed results clearly shows

that the unbound heart tissue concentrations (Figure 10c) most closely predicted the clinically observed ΔΔQTc values at all the time points.

Figure 10. TT 2006 model simulated ΔΔQTc-time (post-dose) profile

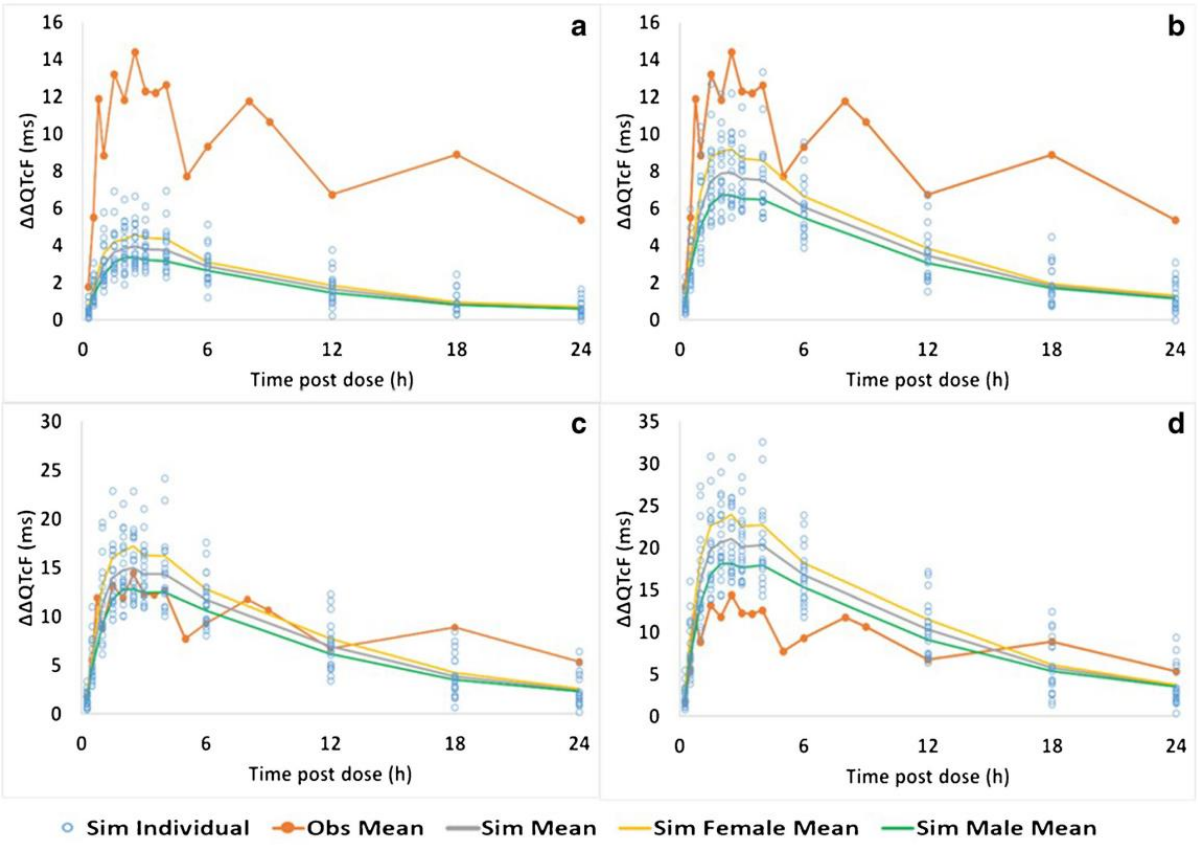

TT 2006 model simulated ΔΔQTc-time (post-dose) profile using (a) unbound plasma, (b) total plasma, (c) unbound heart tissue, and (d) total heart tissue concentrations of MOXI as operational concentration to drive the QT response. The population variability of simulated 20 subjects (open circles), average of the population (thick gray line), average of 10 female population group (yellow line), and average of 10 male population group (green line) are also shown for each of simulation set.

MOXI is considered a potentially torsadogenic drug (38) which is attributed mainly due to its ability to inhibit the hERG channel current. However, the actual reported cases of TdP after MOXI treatment are very rare, which is consistent with the lack of pro-arrhythmic pseudoECG waveforms in any of the virtual patients simulated in Figure 10 as well as the mid-range probability (54%) of being TdP positive as estimated by the Cardiac Risk Algorithm of Polak *et al* (28). Most of the reported TdP cases occurred when MOXI was administered with other cardiotoxic medications potentiating their TdP effect or physiological conditions and diseases such as hypokalemia, tachycardia, renal failure (main route of elimination for MOXI) or

congenital long QT syndrome. Thus, MOXI prolongs the QTc interval at therapeutic dose levels but actual TdP events are contingent upon the presence of other clinical risk factors that may not be present in the healthy volunteer Phase 1 trial setting as simulated.

Hence, to simulate a higher-risk clinical situations, the following scenarios were compared with placebo administration in a virtual 20 years old female subject:

- Scenario 1 – MOXI concentrations equivalent to the mean unbound heart tissue MOXI C_{max} with 400 mg single-dose administration in a healthy individual;
    - Heart rate 60 beats per minute and plasma potassium concentration of 4.2 mM
- Scenario 2 – Supra-therapeutic MOXI concentrations 10-fold higher than the mean unbound heart tissue MOXI C_{max} with 400 mg single-dose administration in a healthy individual;
- Scenario 3 – Therapeutic dosing as in Scenario 1, but simulated in a virtual patient exhibiting pro-arrhythmic physiological factors
    - Tachycardia (heart rate 120 beats per minute) and hypokalemia (plasma K^+ concentration of 1.5 mM)
- Scenario 4 – Supra-therapeutic dosing as in Scenario 2 in a virtual patient exhibiting the same pro-arrhythmic physiological factors as in Scenario 3.

The results of the simulated pseudoECG from the CSS platform are shown in Figure 11 for all scenarios.

Figure 11a shows that under normal physiological conditions (i.e., Scenarios 1 and 2), MOXI prolongs QTc interval without causing any abnormal rhythms even at supra-therapeutic MOXI concentrations. On the other hand, Figure 11b indicates that in the presence of relevant physiological changes (i.e., hypokalemia and tachycardia), the same supra-therapeutic exposure could cause polymorphic arrhythmia. To put in clinical context, the supra-therapeutic MOXI concentration of 120 μM used in Scenarios 2 and 4 is 10-fold higher than the mean unbound heart tissue MOXI C_{max} after 400 mg single oral dose administration. These exposures could be seen in a portion of the patient population under various clinical scenarios, such as drug-drug interactions (viz. inhibition of MOXI clearance), overdose or with intravenous bolus administration of high dose of MOXI (>800 mg). Moreover, patients with renal impairment could show higher exposure at therapeutic doses as MOXI is predominantly cleared by renal filtration, which may underlie the reported TdP cases of MOXI in renally impaired patients

(118). The results show that MOXI, an otherwise low TdP risk drug at therapeutic dose in a healthy subject with normal physiology, could cause TdP when combined with elevated patient physiological risk factors.

Figure 11. Simulated pseudoECG at therapeutic and supra-therapeutic exposure of MOXI

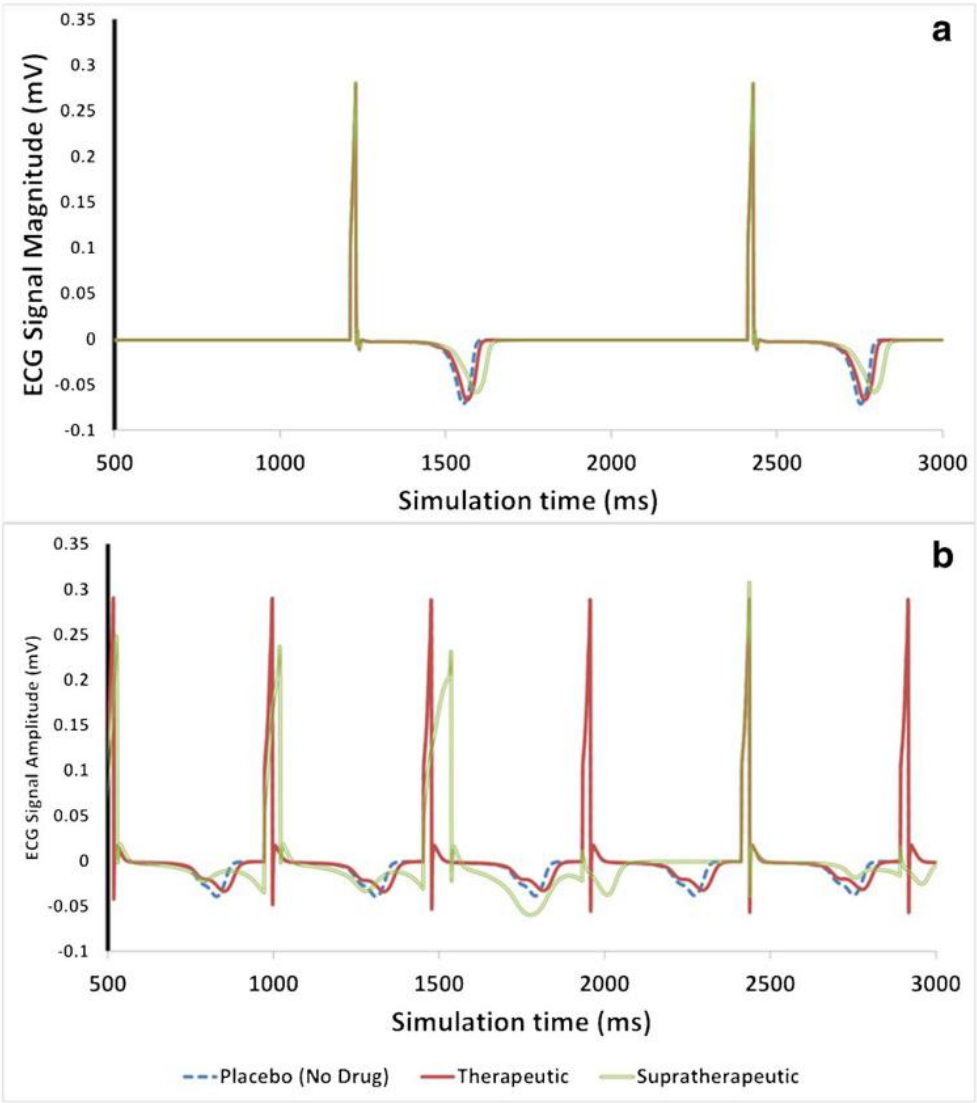

Simulated pseudoECG traces at therapeutic (red thick line), supra-therapeutic (double green continuous line) exposure of MOXI and placebo (no drug) (dotted blue line) under normal physiological conditions (a), and tachycardia with hypokalaemia (b).

PBPK modeling is widely utilized to estimate drug concentrations in various bio-phases for linking with PD models to establish exposure-effect relationships, without the requirement for a direct measurement of drug concentrations at site of action in clinic (119, 120). These models can be semi-or fully-mechanistic and can include multiple physiologically relevant pathways.

For example, the contributions of transporters in lung uptake of MOXI are incorporated based on *in vitro* data, which is important in reproducing the observed clinical lung disposition in tuberculosis patients (53). In the cardiac QST framework, heart tissue concentrations have been established as the relevant bio-phase for governing the QT effect rather than concentrations in plasma per *in vivo* animal work by Minematsu *et al*. (121). However, given that measurement of heart tissue drug concentrations is not feasible in the clinic due to ethical and practical considerations, suitable concentrations to estimate potential cardiac effects in patients are generally not well informed. However, a sufficiently detailed PBPK model that exhibits good predictive performance can potentially help bridge the gap to estimate the concentrations in heart tissue. The robustness of this approach was not fully assessed in the present work, as no clinical or animal data on heart tissue MOXI concentrations was available to verify the PBPK-predicted distribution (i.e., 4-fold higher exposure in heart as compared to plasma). Hence, the model predicted heart tissue MOXI concentration and unbound fraction were used "as is" without further refinement as input to the CSS model and drove the pseudoECG output. This approach demonstrated good predictive performance as shown in Figure 10, where predictions based on the unbound heart tissue MOXI concentration (the most theoretically relevant bio-phase) closely matched the QTc prolongation profile observed in the clinic. Moreover, the CSS model was also able to recover the gender effect in QT prolongation effect, with predicted mean peak ΔΔQTc value ~4.5 ms higher in females than in male subjects and similar to the ~4 ms difference reported by Taubel *et al*. (116). The ability to recapitulate this sex-related difference illustrates an advantage of the model-based QST framework for cardiac risk assessment, as the potential effects of covariates (e.g., food effects, concomitant medications, comorbidities) that affect drug PK and/or PD may be investigated beginning at early development stages.

While the above results indicate that the estimated unbound heart tissue concentration predicted the QT prolongation reasonably well, it is noted that the PBPK model for MOXI is enriched based on non-clinical and clinical PK data which to account for discrepancies between "bottom-up" mechanistic predictions of tissue uptake and clinically observed volume of distribution (viz. application of a Kp scalar). However, simulations such as those presented herein are often conducted during early clinical development, where data is generally more limited and thus there is greater uncertainty in the degree of tissue uptake. This uncertainty was reproduced herein as multiple potentially relevant bio-phase concentrations were considered to generate plausible CSS outputs reflecting a ~5-fold range of mean peak ΔΔQTc values (i.e.,

ranging from approximately +4 ms to +20 ms for unbound plasma and total heart MOXI concentrations, respectively). Such an approach is useful in early development, where a set of predictions reflecting a range of potential clinical scenarios may be highly informative in cardiac risk assessment, clinical trial design and overall clinical development strategy. Even though it was attempted to develop the most mechanistically plausible model based on currently available knowledge in the area, it is worth noting the uncertainties and assumptions associated with the model and input data for the novice in the field. For example, the model did not explicitly model formulation effects such as over-encapsulation because such information is rarely made publically available and clearly not well defined in the clinical studies used for model verification. Secondly, a fully detailed heart tissue model to mimic the exposure inside the cardiomyocyte cell was not available, which has been suggested to be more suitable exposure for some compounds (122-124). Such detailed heart tissue models exist (125, 126) however they could be even more challenging to verify with limited measurements in heart tissue or cardiomyocytes and the *in vitro* IC_{50} data also reflects the concentration in the media not inside the cell thus combining such IC_{50} without suitable correction with intra-cellular exposure model could produce misleading results. The relevance of *in vitro* experiments, typically conducted in HEK cells with heterologously expressed cardiac ion channels, to the *in vivo* situations or actual cardiomyocytes in terms of physiological functions is not fully established. Nonetheless, these are the challenges facing the general cardiotoxicity assessment area rather than this manuscript specifically and more experimental data is required to complement such modelling results to test or establish hypotheses and move the field of cardiac risk assessment forward.

Although the estimated unbound heart tissue MOXI concentrations resulted in the best match to the observed clinical data when used as the input for the CSS model, it is noted that PK-PD relationships for cardiac parameters (e.g. QT prolongation) are predominantly reported as correlations with plasma drug concentrations. This correlation is shown in Figure 12, which depicts the ΔΔQTc values predicted from the CSS using unbound heart tissue MOXI concentration as input versus concentrations at the corresponding time points (unbound heart tissue and total plasma MOXI concentrations in open and closed circles, respectively).

Figure 12. Relationship between simulated MOXI concentrations and ΔΔQTcF

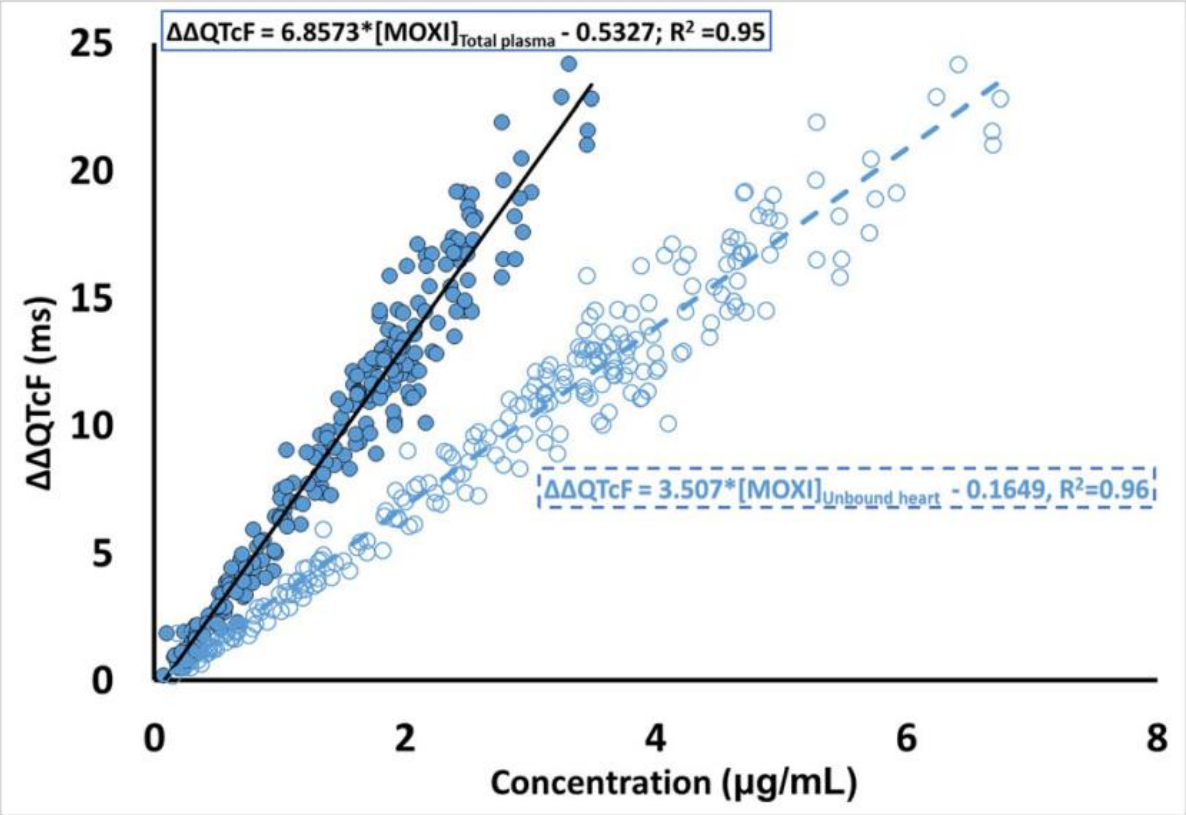

Relationship between simulated MOXI concentrations and ΔΔQTcF (filled blue circles represent the total plasma concentration vs. ΔΔQTcF obtained with unbound heart tissue concentration as operating concentration and open blue circles represent the unbound heart tissue concentration vs. ΔΔQTcF obtained with unbound heart tissue concentration as operating concentration).

Figure 12 show robust correlations with the predicted ΔΔQTcF, with slopes of 6.86 and 3.51 ms per µg×mL^{-1} of MOXI in total plasma and unbound heart tissue bio-phases, respectively, with the steeper slope for the plasma correlation reflecting the lower MOXI concentrations in the total plasma vs. the unbound heart tissue bio-phases. Notably, when compared with published slopes from clinical studies, the "bottom-up" predicted slope of 6.86 ms per µg×mL^{-1} for the plasma correlation was similar to slightly higher in magnitude. For example, the value reported by Panicker *et al*. (115) from a bootstrapping analysis was 5.9 ms per µg×mL^{-1}, whereas an earlier population PK-PD study by Florian *et al*. reported slopes from individual studies ranging from 1.6 to 4.8 ms per µg×mL^{-1} and a mean estimate of 3.1 ms per µg×mL^{-1} (111). In the latter case, it is noted that this may be influenced by clinical trial size, as clinical studies with larger populations are known to have slopes higher than 3.1 ms per µg×mL^{-1} (127). Regardless, this suggests that the bottom-up approach outlined in the present

work provides reasonable, if possibly somewhat conservative, predictions of QTc prolongation for MOXI.

Although the ΔΔQTcF is a useful comparator for evaluating performance of the PBPK-based CSS simulations, it is important to note that the reliance on QTc as a metric of torsadogenic potential has significant drawbacks (22, 128). This is exemplified by MOXI, as reports by Abbasi *et al* (31), Okada *et al*. (48) and simulations done previously by our group (28) have shown with single cell level as well as 3D heart wall simulations that MOXI doesn't cause early after depolarization (EAD) or arrhythmia at up to 100-fold supra-therapeutic concentration with healthy cardiac electrophysiology. While this is in contradiction to the reported TdP cases with MOXI in clinic at lower than 100-fold exposure levels (129, 130), these cases, as well as 274 records of MOXI-associated TdP (obtained by mining of the US FAERS database using the OpenVigil 2.1 portal (131) for TdP cases reported with MOXI) indicates that almost all cases were multifactorial. Specifically, the MOXI-associated cases involved other contributing factors, such as additional QT prolonging co-medications, disease conditions such as renal failure or physiology modifications that could influence cardiac electrophysiology such as electrolyte imbalance or abnormal heart rate. It should be emphasized that these findings are highly consistent with pseudoECG simulations presented herein, which also show that MOXI itself is less likely to cause TdP even at 10-fold higher than therapeutic exposure in a healthy subject but could cause arrhythmia when administered to patients with other physiological risk factors or co-medications with torsadogenic potential (refer to Figure 11). Hence, this demonstrates that the application of the cardiac QST modelling framework shown in this study could potentially help bridge the translational gap by starting with assumption rich exploratory simulations in early clinical development with iterative refinement through learn-confirm-predict cycles through later stages of drug development. Such an approach is envisioned to guide both appropriate labelling and rational pharmacotherapy of new drugs to avoid or reduce post-marketing TdP risk.

4.3.2. Differences in reported IKr IC50 values and its impact on QST model prediction:

Lab to lab variability in cell based *in vitro* assays, such as those used to provide input values for use in the present analysis, is well documented (39, 132). This can be seen in the reported IKr IC50 values of MOXI from different laboratories and different experimental protocols provided in Table I as well as in the results of an extensive literature search carried out for IC50 values of many drugs and drug-like compounds for various cardiac ion channels (available on

tox-database.net) (39). However, despite the known variability in lab-based parameters which can potentially strongly influence QST modelling outputs, the impact of this variability is not commonly assessed and reported. To minimize the effects of such variability within the current study, a step-wise strategy was applied to identify the most physiologically relevant experimental input value of IC50 for QST modelling. Results were first triaged based on cell line, where HEK cells were preferred over CHO cell or other non-human cell lines due to their human origin. Of those based on HEK cells, Alexandrou *et al*. (40) and Chen *et al*. (73) used the same experimental protocols, mimicking human physiology with minor difference in operating temperatures. While Lacroix and colleagues (77) have also run their study in the physiological temperature, there were other settings that differed from human physiology (higher value of the holding potential and short pulses) which resulted in their removal from consideration.

Of the remaining two studies, as the experimental conditions used by Alexandrou *et al*. (40) were the most physiologically relevant, their reported IC_{50} value of 29 μM was used for all the simulation results presented in this publication. However, it is noted that the experimental conditions were very similar differing only in experimental temperature (35-37 vs. 34-36 ^{o}C; Alexandrou *et al*. (40) and Chen *et al*. (73), respectively). While these differences appear minor, Table I shows that even small temperature changes may have resulted in an approximately 20% difference in IC50 values, albeit inter-lab, inter-operator or even inter-run variability may also contribute to the differences. These sources of variability, which seem to be typical for the Patch Clamp technique, may influence decisions taken on the cardiac safety assessment (132). To evaluate the potential impact of the input IC_{50} value on the model predictions, a sensitivity analysis conducted to study the impact of varying the IC_{50} from 1 to 300 μM on ΔΔQTcF was conducted (Figure 13).

An IC_{50} of around 30 μM, similar to the 29 and 35 μM values from Alexandrou *et al*. (40) and Chen *et al*. (73), gave the predicted ΔΔQTcF closest to clinically observed. In contrast, higher values as estimated under less physiologically-relevant conditions, would have under-predicted the magnitude of QTc prolongation. Thus, it is very important to supply the *in vitro* input parameters obtained from the experiments conducted at operating conditions mimicking *in vivo* situations as quality of QSTS prediction depends heavily on the quality of input information supplied to mechanistic model.

Figure 13. Sensitivity analysis of predicted ΔΔQTcF with respect to IKr IC_{50} value for MOXI

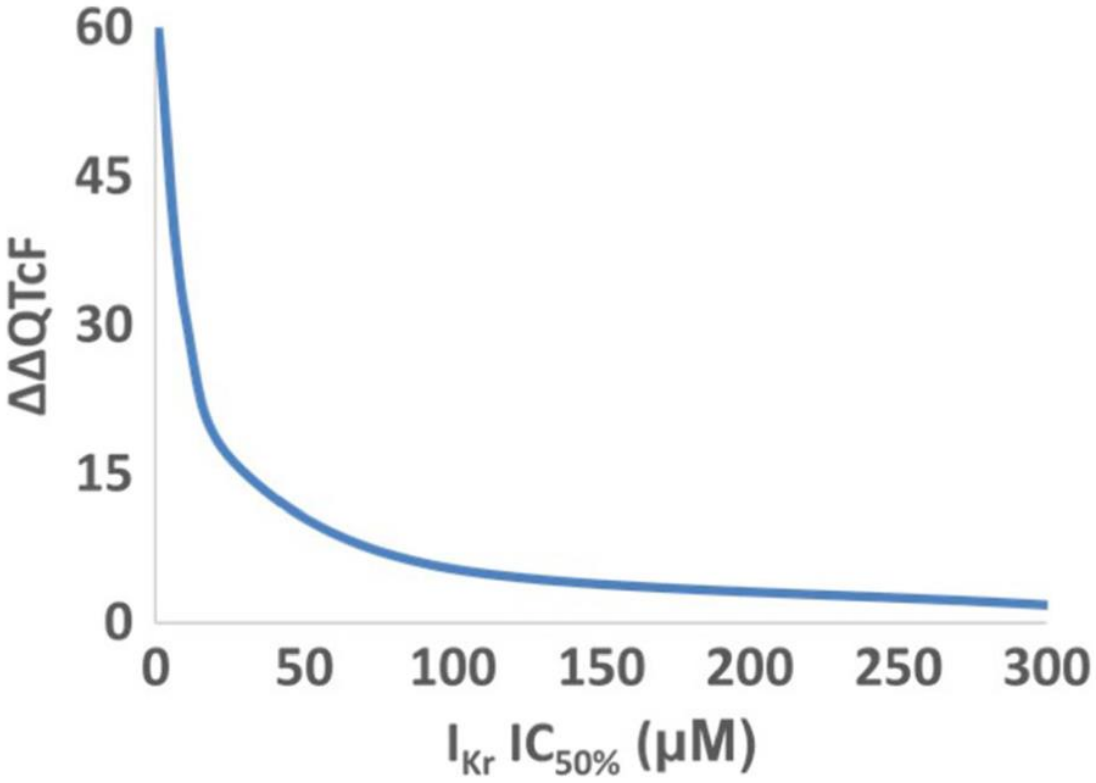

It is noted that to aid in translation of IC50 values obtained from different cell lines and different temperatures, the CSS contains validated mathematical inter-system scaling factors (ISSF) (133). However, these factors are only intended to help correct values to better match human physiology, and as such the ISSF should be used cautiously as they are not intended to replace physiologically-relevant *in vitro* experimentation.

4.3.3. Impact of model selection on the model outcomes:

The TT2006 model was primarily used to run the pseudoECG simulations in the current work, given the existence of numerous peer-reviewed publication demonstrating its utility in adequately predicting the clinically observed QT prolongation. This model is also relatively fast to run, especially at the pseudoECG level. However, the ORd model and its variants (122, 134) have recently been proposed as a method to run single cell simulations to propagate the impact of *in vitro* IC_{50} value of ion current inhibition to action potential duration (APD). Although the ORd model to run the pseudoECG simulations offers some additional insights, its overall impact to this work remains limited or negligible, when compared to the use of the TT2006 model. Moreover, the simulations with the ORd model takes significantly longer time and shows some numerical instability at pseudoECG level in some individuals, when running

simulations unbound plasma and unbound heart tissue concentration exposure. Thorough evaluations of available cardiomyocyte models in terms of the numerical accuracy and their ability to recover observed APD and/or ECG signals is needed to establish the utility of the models to simulate clinical endpoints and/or regulatory use such as CiPA initiative. The impact of model selection on our results is shown in Figure 14.

Figure 14. ORd and TT2006 model comparison in terms of predicted *ΔΔQTc-time profile*

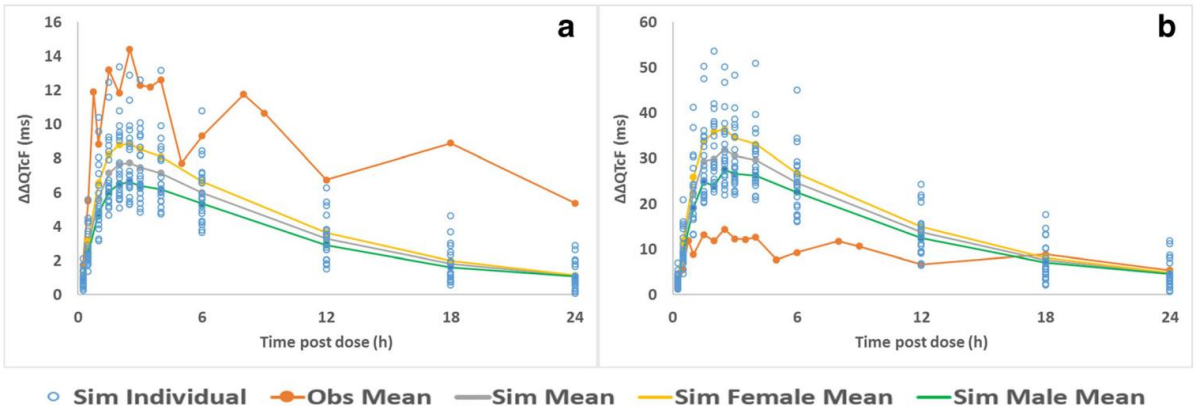

ORd model simulated ΔΔQTc-time (post dose) profile using A) unbound plasma; and B) unbound heart tissue concentrations of MOXI as operational concentration to drive the QT response. The population variability of simulated 20 subjects (open circles); average of the population (thick grey line); average of 10 female population group (yellow line) and average of 10 male population group (green line) are also shown for each of simulation set.

The ORd model resulted in larger QT prolongation estimates as compared to the TT2006 model, at the same exposure levels [Figures 10 and 14]. The ORd model showed over- and under-estimation of clinically observed QT prolongation profile of MOXI with unbound heart and unbound plasma concentrations, respectively. As such, it is likely that the observed QT prolongation profile is more adequately matched to the total plasma exposure with the ORd model, while the TT2006 model showed best predictions with unbound heart tissue concentrations. As stated above, the aim of the current study was to test physiologically plausible scenarios therefore; this work does not focus on total plasma concentrations, which would deviate from the hypothesis that only the free drug can be pharmacologically active. Further experimental and *in silico* work is needed to determine and establish the utility and/or accuracy of various QST models and input data choices to continuously grow the current knowledge base.

4.4. Application of QSTS approach in post marketing surveillance (Phase IV):

A QSTS model for CT was established to simulate, *in silico*, a 'virtual twin' of a real patient to predict the occurrence of cardiotoxic events previously reported in patients under various clinical conditions. The QSTS model considered the effects of CT and its most notable electro-physiologically active primary (DCT) and secondary (DDCT) metabolites, on cardiac electrophysiology. The *in vitro* cardiac ion channel current inhibition data was coupled with the biophysically detailed model of human cardiac electrophysiology to investigate the impact of (1) the inhibition of multiple ion currents (I_{Kr}, I_{Ks}, I_{CaL}); (2) the inclusion of metabolites in the QSTS model and (3) unbound or total plasma as the operating drug concentration, in predicting clinically observed QT prolongation. The inclusion of multiple ion channel current inhibition and metabolites in the simulation with unbound plasma CT concentration provided the lowest prediction error. The predictive performance of the model was verified with three additional therapeutic and supra-therapeutic drug exposure clinical cases. The results indicate that considering only the hERG ion channel inhibition of just the parent drug is potentially misleading, and the inclusion of active metabolite data and the influence of other ion channel currents should be considered to improve the prediction of potential cardiac toxicity. Mechanistic modelling can help bridge the gaps existing in the quantitative translation from preclinical cardiac safety assessment to clinical toxicology. Moreover, this study shows that the QST models, in combination with appropriate drug and systems parameters, can pave the way towards personalised safety assessment.

CT is one of the most widely prescribed antidepressant drugs (135). It has been linked with cardiac toxicity (especially at higher doses) resulting in the US FDA advocating restrictions on the maximum daily dose in 2011 (87) and further restrictions to the recommended dosage in special populations in 2012 (92). Cardiac safety concerns associated with CT were documented prior to the 2011 FDA warning. In fact, the clinical development of the drug was halted in the 1980s due to the sudden unexplained deaths of dogs who were administered CT as part of high dose toxicity studies (25). Later, as part of a detailed evaluation, the torsadogenic potential of the secondary metabolite of CT, DDCT, was investigated. Following CT dosing, the metabolite DDCT was found at high levels in dogs but not in other species studied, including humans due to species specific metabolic differences (25). There is evidence suggesting that CT inhibits multiple cardiac ion currents: IKr (rapidly activating delayed rectifier potassium channel current) (94), IKs (slowly activating delayed rectifier potassium channel current) (94), and ICaL (late calcium channel current) (95, 136), it is also suspected to interfere with additional

ionic channels and currents (137). Furthermore, the primary metabolite DCT and secondary metabolite (DDCT) are also known to inhibit IKr and IKs currents (94). DDCT is only detectable in human blood following the administration of high CT doses. The peak in the level of DDCT typically occurs several hours after the ingestion of high doses of CT. The cardiotoxicity is also observed much later after ingestion of high doses of CT which can be attributed to the delayed formation and accumulation of DDCT following high CT dose administration (138). However, DDCT is not the only toxicity factor involved, since high concentrations of CT can also affect cardiac function by modifying the electrophysiology of the heart via the central nervous system (CNS). This complex interplay of the parent drug, its metabolites, and the inhibitory effect on multiple cardiac ion channels may all contribute to the continued debate on the cardiac safety associated with CT (92, 139-141). Until recently, torsadogenicity assessments were typically focused on the inhibition of the cardiac IKr current occurring at the level of the hERG channel (encoded by the human ether-a-go-go gene) (29, 31, 142, 143). Over the last few years, the comprehensive *in vitro* proarrythmia assay (CiPA) initiative has been advocating the *in vitro* assessment of multiple cardiac ion currents and the estimation of the combined effect of multiple ionic channel inhibition using cardiomyocyte cell based quantitative systems models (144, 145). However, the primary focus of the CiPA has been on the parent drug, specifically at the single cardiac cell level (146). Assessment of the QT prolongation liability of a drug based only on the parent drug and the hERG centric evaluations could be misleading since many drugs such as CT affect not only I_{Kr} but also other ionic currents and may have electro-physiologically active metabolites (142, 147). Testing all probable hypotheses in clinical and/or animal studies may be practically, ethically and economically unfeasible (25). Therefore, modelling and simulation methods can complement experimental studies and reduce and/or refine the number of performed experiments. In this study the ability of the biophysically-detailed models of cardiac electrophysiology was studied, parameterized with *in vitro* cardiac ion channel inhibition data, to predict the QT prolongation observed clinically at various exposure levels and under varied clinical scenarios. The following scientific questions were investigated to explain the observed QT prolongation with CT administration at therapeutic and supra-therapeutic concentrations (up to 100-fold higher): (i) is the parent drug (CT) exclusively responsible for the observed QT prolongation? (ii) is the I_{Kr} (hERG) inhibition activity by all chemical moieties (CT, DCT, and DDCT) the only ion current that causes the observed clinical cardiotoxic events? (iii) what is the operating concentration of drug and metabolites to drive the cardiac response - unbound plasma or total plasma concentration? Most of the systems toxicology models are established and verified

based on the average response of a population or a trend. Using quantitative system modelling, here we assessed the potential of actually simulating the 'virtual twin' (148) of a real patient, considering their physiology and specific clinical conditions (drug exposure, heart rate, etc.). The resulting cardiotoxic event was then predicted for a given individual under specified conditions *in silico*. The meaning of a 'virtual twin' could be different in clinical literature (149), so for our study we refer to a 'virtual twin' as an *in silico* model with systems (physiology) parameters mimicking an individual patient under given clinical circumstances that allows simulation of the clinical response/outcome of interest for that patient. Hence we conducted a thorough literature to identify the reported clinical cases of TdP associated with CT in which there were no known physiological diseases (e.g., cirrhosis) or medications (e.g., metabolic drug-drug interactions) that could alter disposition of CT. To avoid bias, cases were identified where maximum possible data on pharmacokinetics and patient electro-physiology information was measured in clinic. Literature search was conducted and review via PubMed, Google Scholar and citation within some review articles and could identify three clinical case reports which presented the occurrence of actual cardiotoxic events following the ingestion of CT where drug concentrations, patient demographics and heart rate parameters, and clinical conditions (e.g. plasma electrolyte concentrations) were measured for us to closely mimic the real clinical scenario (84-86). Most of these reports were overdose situations hence to verify the QSTS model QT prolongation at therapeutic dose of 20mg was also simulated and compared with corresponding clinical data although matching set of measured drug concentration, QT prolongation and heart rate was not available from single study at therapeutic dose level. Additional heart wall physiology parameters which are not commonly measured in routine clinical trials such as ventricular heart wall thickness, cardiomoycytes size, etc.; were either calculated from age and gender of patient using known covariate models or assumed based on known values of that parameter for a healthy Caucasian population. The simulation results were compared with clinically observed QT prolongation or TdP. Utilization of quantitative systems models to simulate absorption, distribution and elimination of a single drug or combination of drugs, generally referred to as PBPK models, have already been well established in defining or refining appropriate dosage recommendations in regulatory submissions (150-153). However, utilization of such a quantitative systems approach to simulate therapeutic response or toxicity events is not widely explored, probably due to the limited availability of sufficiently verified systems toxicology models and/or the availability of suitable input and quantitative systems (physiology) data to parameterize the model. Here a QSTS model was employed to predict drug cardiotoxicity, namely QT prolongation, after

therapeutic and supra-therapeutic dosing of CT. Verification of the predictive performance of the model was done against four different clinical datasets of varying demographics and physiological conditions.

The simulated QT and QTc for all four clinical cases (CASE I-IV) and ten simulated exposure data points for five different scenarios (SIM 1-5) along with corresponding clinical observations are summarized in Table 7.

Table 7. Observed and Predicted QT Interval or Prolongation (in Milliseconds) After Administration of Various Doses of CT

Case	Exposure ID	Observed			Predicted									
					All moieties multiple channels				Free Plasma Concentration					
					Free plasma		Total plasma		All moieties only I_{Kr}		Only CT only I_{Kr}		Only CT multiple channels	
					SIM 1		SIM 2		SIM 3		SIM 4		SIM 5	
		QT (ms)	RR (s)	QTcB (ms)	QTcB (ms)	AE (ms)	QTcB (ms)	AE (ms)	QTcB (ms)	AE (ms)	QTcB (ms)	AE (ms)	QTcB (ms)	AE (ms)
Case I[a]	S1E1	460	0.74	535	538	3	618	83	499	36	481	54	484	51
	S1E2	460	0.83	505	495	10	576	71	465	40	452	53	455	50
	S1E3	440	0.74	511	513	2	589	78	486	25	473	38	475	36
	S1E4	420	0.78	476	483	7	536	60	413	63	404	72	404	72
	S1E5	380	0.78	430	438	8	438	8	438	8	438	8	438	8
AAE (ms)						6		60		34.4		45		43.4
Case II[a]	S2E1	NA	0.4–0.6	572–600	597	11	624	38	577	9	566	20	569	17
Case III[a]	S3E1	440	0.531	604	CNC		CNC							
	S3E2	600	0.8	671	641	30	737	66						
	S3E3	420	0.428	642	CNC		CNC							
Case IV[b,c]	S4E1	NA	NA	8.5	9.53	1.03	21.93	13.43						

CNC cannot calculate due to a metamorphic ECG trace which can be inferred as arrhythmia as in the actual clinical study, *NA* not available, *AE* is the absolute error in prediction, *AAE* is the average absolute error for a given case study, *RR* is the time interval in seconds between two consecutive R waves on the ECG trace which also represents heart rate, *QTcB* is the QT interval in ms corrected for heart rate by Bazzett's formulae, *ID* identification, *CT* citalopram, SIMs 1–5 simulations 1–5

[a] Predicted is an average of five simulations for a given individual (see supplementary material for inter-occasion variability generated in heart rate and plasma electrolyte concentrations and simulated pseudoECG)

[b] Average value of a population in clinical and simulation studies

[c] Prolongation in QTcF interval (in ms) from drug as compared to placebo (ΔQTcF)

Absolute error (AE) in prediction [Abs(OBS-PRED)] and average absolute error (AAE) are reported for each case where the observed data allowed to accurately calculate the errors. For all cases (CASE I – IV) and exposure levels, the SIM 1 simulation scenario setting has consistently provided the lowest prediction error with respect to clinically reported QT prolongation. All simulation scenarios (SIM 1- 5) for CASE I and CASE II were tested to establish our hypothesis and then simulated only the SIM 1 and SIM 2 settings for the remaining two cases (CASE III and CASE IV) to verify the hypothesis. Since CASE I is the richest in terms of data points, the average absolute error (AAE) was also reported for easier comparison of various settings (SIM 1-5).

The predicted QTc for all five time points of CASE I with different simulation settings (SIM 1-5) are shown along with clinical QTc in Figure 15. It is evident from Figure 15 and Table 7 that when parent and both metabolites effect on all three cardiac ion currents were accounted for with unbound plasma concentration as operating concentration to drive response, the predictions were closest to the clinical data. The actual QT was not reported in CASE IV hence the average ΔQTcF of the simulated population was compared with the population mean ΔQTc reported in the clinical study report to calculate the prediction error.

Figure 15. Comparison of simulated QTcB interval with different simulation settings (SIM 1–SIM 5) at five different exposure levels (S1E1–S1E5) of case I

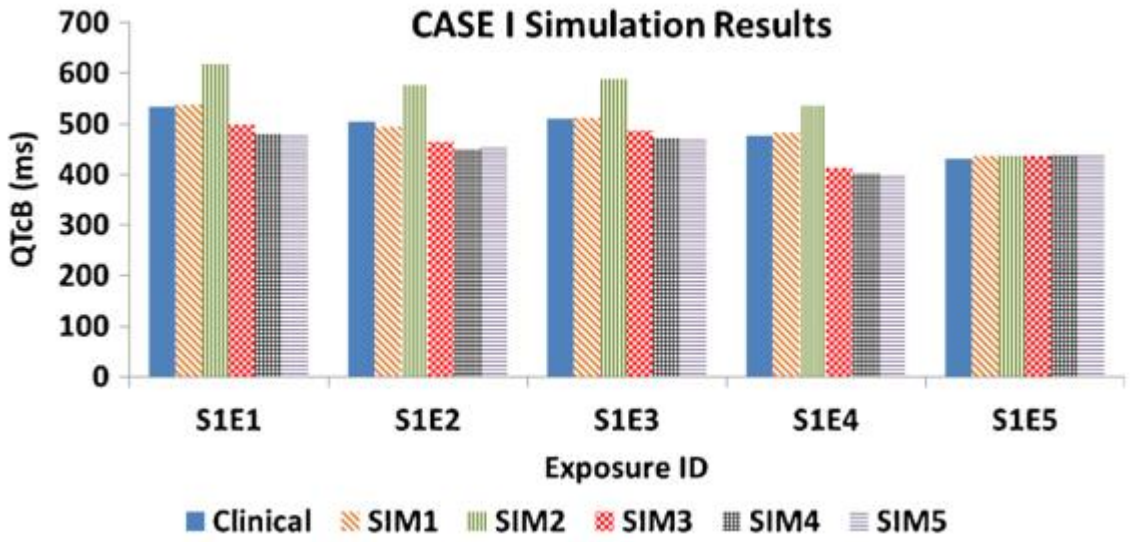

CASE I records the highest number of clinical measurements (i.e. drug concentration with matching QT and RR interval for four different time points after CT ingestion) providing the most comprehensive scenario for verifying our hypotheses (86). Five different simulations (SIM 1 – SIM 5) were run with various combinations of responsible moieties, ion channels and operating concentrations as specified in the Methods section. The results are shown in Figure 15 and Table 7. The simulated results showed that when free plasma concentrations of all three entities (CT, DCT and DDCT) and multiple ion channel interactions were considered (SIM 1), the simulated QTcB (QT interval corrected for heart rate by Bazett's correction) (154) showed the lowest AAE (Table 7). Bazett's correction method was used to match the reported QTc in the clinical study report. The heart rate (as RR interval) is provided in Table 7 hence an interested reader can apply any other heart rate correction formulae e.g. Fridericia and compare the results, however the choice of correction formulae was highly unlikely to influence our conclusions. When total plasma concentrations were used as the operating concentration with

all moieties, and all ion channel interactions were considered (SIM 2), the QT prolongation was over-predicted. PseudoECG traces of SIM 1 and SIM 2 scenarios compared to placebo (zero drug and metabolite concentrations) over a period of 10 seconds are shown in Figure 16. QT interval from the ECG signals was automatically calculated by an inbuilt algorithm within the CSS platform and reported in the Table 7.

When we used free plasma concentration as the operating concentration and all moieties with only hERG inhibition (SIM 3), the model under-predicted the effect hence it appears that the inclusion of the IKs current is important. When the effect of metabolites was neglected by simulating only the parent (CT) concentration with either only IKr (SIM 4) or with multiple ion channels (SIM 5), the model under-predicted the observed QTcB indicating the significant contribution of metabolites (especially that of DDCT which is clinically important as a potent IKs current inhibitor). Thus the simulation result of CASE I indicates that consideration of metabolites, together with parent drug and multiple ion channels, is important in the accurate prediction of QT prolongation after CT ingestion (Table 7, Figure 15).

However, it is worth noting that the established model has several key assumptions:

- A 1D model of the ventricular heart wall is sufficient to simulate the clinical ECG signal which is a three dimensional phenomenon in reality;
- The parent to metabolite ratios obtained at a 20mg CT dose level are valid at supra-therapeutic dose levels. Studies by Unterecker *et al*. (86) and Liotier & Coudoré (84) showed a linear elimination phase of CT plasma concentration profiles at supra-therapeutic doses, probably indicating non-saturable clearance at the studied dose ranges;
- The combined effect of parent and metabolite on various ion channel currents is additive;
- In absence of measured/estimated heart tissue concentrations, the CT plasma concentrations are considered the effective drug exposure driving the cardiac response, while other reports suggest that the heart tissue concentration is a better surrogate drug exposure driving the cardiac response (121, 126, 155);
- Plasma protein binding is non-saturable for the studied drug concentrations.

Figure 16. PseudoECG trace over a 10-s period for S1E1 exposure level with free plasma (SIM 1) or total plasma (SIM 2) concentrations

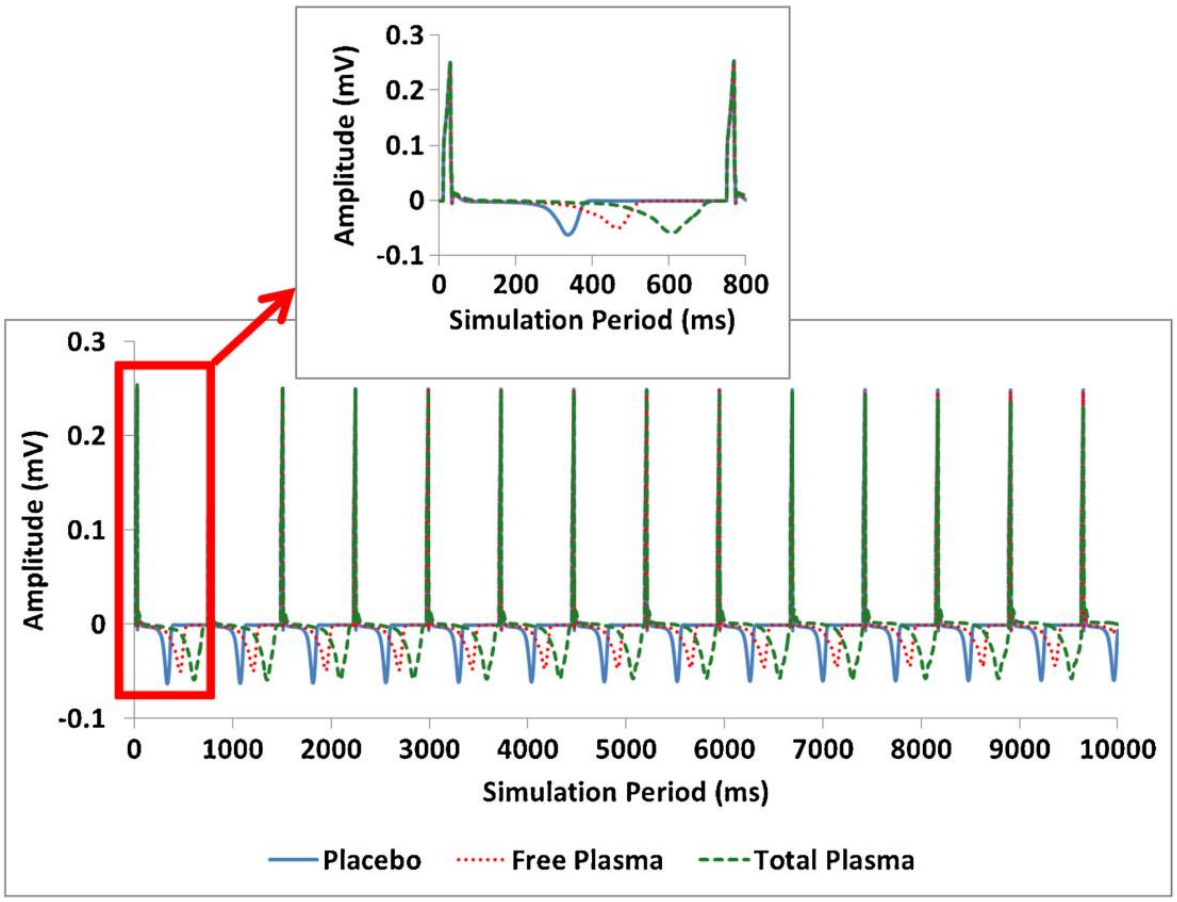

With several assumptions and uncertainties described, to build more confidence in the model, a further three clinical scenarios were used to see if the same model can also explain other observed clinical outcomes. The model was tested using data collated from other clinical studies; QT prolongation at a therapeutic dose of 20 mg and two more cardiotoxicity case reports describing a CT overdose (84, 85). The results consistently indicated that considering all moieties (CT, DCT and DDCT) and multiple ion channel interactions with free plasma concentration as the operating concentration is crucial in the prediction of an accurate cardiotoxicity profile of CT at therapeutic and supra-therapeutic doses (Table 7). The pseudoECG trace simulated for the Liotier & Coudoré 2011 study (CASE III) was morphologically erratic and the signal analysis module implemented within the CSS platform was not able to calculate the QT interval using the default automated QT interval calculation algorithm [Figure 16]. It was hypothesized that the erratic pseudoECG signal was the effect of a combination of high concentrations of active moieties, rapid heart rate and hypokalemia (84). The observation of clinical ECG traces in the clinical study report appears to show deviation

from the standard rhythm of an ECG signal. However, the clinical study reported a QT interval probably from the manual reading of the observed QT interval taken from the erratic ECG profile. The simulations were able to predict the erratic ECG signal of this clinical scenario although comparison of the QT interval was not possible since the automatic calculation of QT interval in the model could not be performed due to the erratic and non-physiological simulated ECG traces (Figure 16). It could be read manually from the predicted native ECG traces, however a manual interpretation of the pseudoECG signal into the QT interval was not performed.

The systems cardiotoxicity model for CT was established and verified the predictive performance of the model against four different clinical studies at different dose levels and physiological conditions to improve confidence in our findings. A simulation set up was identified that consistently explained the observed QT prolongations, at all dose levels, as the plausible mechanism of the QT prolongation of CT. Mechanistic models are useful tools for assessing hypotheses and understanding mechanisms of toxicity which are otherwise difficult or practically impossible to study *in vivo*. For example, it is difficult to only study the effect of CT *in vivo* since the drug is converted to the metabolite DCT via multiple metabolic pathways and then rapidly transformed to DDCT hence all three moieties exist and exert their effects simultaneously, blocking multiple ion channels. In contrast, accurately parametrized and sufficiently qualified physiologically based models can be used to conduct various simulations to investigate "what-if?" scenarios for understanding or establishing the underlying mechanisms and for investigating the effect of each contributing factor.

The current study also highlights the application of population-based biophysically-detailed models of cardiac electrophysiology to simulate real patients within a virtual environment providing the possibility of applying such approaches towards personalised medicine and therapeutics. For example, with the use of such mechanistic modelling approaches in combination with infrequent clinical measurements, one can estimate when the plasma concentrations in an overdosed patient return to safe levels and also assess when the safety biomarkers (e.g. QTc) are expected to reach safe levels. This individual patient-centred assessment procedure could allow the medical staff to estimate the duration of hospitalisation, potentially replacing the current frequent blood sampling and clinical marker measurements to assess the recovery of the patient.

The results of this study indicate that considering only hERG ion channel inhibition of the parent drug, when predicting cardiotoxicity, may not provide reliable predictions. Where possible, the inclusion of active metabolite data and the influence of other ion channel currents should be considered for a better prediction of potential cardiac toxicity. Mechanistic modelling can help fill the current gaps in the quantitative translation of preclinical cardiac safety assessment to clinical toxicology. Population-based biophysically-detailed models can potentially be used in personalised therapeutics, and the mathematical models based around the 'virtual twin' concept should be considered as one of the approaches towards such bespoke patient therapies.

5. Conclusions

The assessment of pro-arrhythmic potential and risk of TdP of novel molecules is often challenging given the complex interplay of multiple factors involved requiring a comprehensive understanding of not only the drug dependent parameters but also the systems characteristics such as human anatomy, physiology, and pathophysiology, as well as external factors e.g., dosing scheme, concomitantly taken drugs, co-morbidities, etc. While the method demonstrated herein appears to predict the cardiotoxicity for a well-characterized drugs reasonably well, it is envisioned that QSTS modelling be applied throughout development where the component models are refined iteratively through further study per the "learn-confirm-predict-apply" paradigm with enrichment of clinical knowledge of the compound in order to guide decision making during drug development. Application of a progressive QSTS cardiac risk assessment paradigm starting in early development could guide drug development decisions and later define a clinical "safe space" for post-approval risk management to identify high-risk clinical scenarios. Additional collaborative initiatives are needed to further understand the impact of input data sources and model selections toward establishing good practices to progress the field forward. Further work demonstrating the performance of the QST framework for other drugs and different formulations, routes of administration, co-medications and diets as well as in the recapitulation of real TdP cases would help to validate this approach and build confidence in proposed progressive risk assessment strategy.

6. References

1. Piccini JP, Whellan DJ, Berridge BR, Finkle JK, Pettit SD, Stockbridge N, et al. Current challenges in the evaluation of cardiac safety during drug development: translational medicine meets the Critical Path Initiative. American heart journal. 2009;158(3):317.

2. Redfern W, Ewart L, Hammond T, Bialecki R, Kinter L, Lindgren S, et al. Impact and frequency of different toxicities throughout the pharmaceutical life cycle. The Toxicologist. 2010;114(S1):1081.

3. Laverty HG, Benson C, Cartwright EJ, Cross MJ, Garland C, Hammond T, et al. How can we improve our understanding of cardiovascular safety liabilities to develop safer medicines? British Journal of Pharmacology. 2011;163(4):675-93. doi: 10.1111/j.1476-5381.2011.01255.x.

4. Stockbridge N, Morganroth J, Shah RR, Garnett C. Dealing with Global Safety Issues. Drug Safety. 2013:1-16.

5. Guideline I. E14. The Clinical Evaluation of QT/QTc Interval Prolongation and Proarrhythmic Potential for Non-Antiarrhythmic Drugs. May 2005.

6. Hondeghem L. QTc prolongation as a surrogate for drug-induced arrhythmias: fact or fallacy? Acta cardiologica. 2011;66(6):685.

7. Yap YG, Camm AJ. Drug induced QT prolongation and torsades de pointes. Heart. 2003;89(11):1363-72.

8. Guth BD, Germeyer S, Kolb W, Markert M. Developing a strategy for the nonclinical assessment of proarrhythmic risk of pharmaceuticals due to prolonged ventricular repolarization. Journal of Pharmacological and Toxicological Methods. 2004;49(3):159-69.

9. Mendyk A, Wisniowska B, Fijorek K, Glinka A, Polak M, Szlek J, et al., editors. Empirical modeling of the sodium channel inhibition caused by drugs. Computing in Cardiology (CinC), 2012; 2012: IEEE.

10. Polak S, Wiśniowska B, Ahamadi M, Mendyk A. Prediction of the hERG potassium channel inhibition potential with use of artificial neural networks. Applied Soft Computing. 2011;11(2):2611-7.

11. Polak S, Wiśniowska B, Glinka A, Fijorek K, Mendyk A. Slow delayed rectifying potassium current (IKs)–analysis of the in vitro inhibition data and predictive model development. Journal of Applied Toxicology. 2012.

12. Wiśniowska B, Mendyk A, Fijorek K, Glinka A, Polak S. Predictive model for L-type channel inhibition: multichannel block in QT prolongation risk assessment. Journal of Applied Toxicology. 2012;32(10):858-66.

13. Du L, Li M, You Q, Xia L. A novel structure-based virtual screening model for the hERG channel blockers. Biochemical and biophysical research communications. 2007;355(4):889-94.

14. Thai K-M, Ecker GF. A binary QSAR model for classification of hERG potassium channel blockers. Bioorganic & medicinal chemistry. 2008;16(7):4107-19.

15. Champeroux P, Viaud K, El Amrani AI, Fowler JSL, Martel E, Le Guennec JY, et al. Prediction of the risk of torsade de pointes using the model of isolated canine Purkinje fibres. British Journal of Pharmacology. 2005;144(3):376-85.

16. Antoons G, Oros A, Beekman JD, Engelen MA, Houtman MJ, Belardinelli L, et al. Late Na+ current inhibition by ranolazine reduces torsades de pointes in the chronic atrioventricular block dog model. Journal of the American College of Cardiology. 2010;55(8):801-9.

17. Cheng HC, Incardona J. Models of torsades de pointes: effects of FPL64176, DPI201106, dofetilide, and chromanol 293B in isolated rabbit and guinea pig hearts. Journal of Pharmacological and Toxicological Methods. 2009;60(2):174.

18. Fridericia LS. Die Systolendauer im Elektrokardiogramm bei normalen Menschen und bei Herzkranken. Journal of Internal Medicine. 1920;53(1):469-86.

19. Yao X, Anderson D, Ross S, Lang D, Desai B, Cooper D, et al. Predicting QT prolongation in humans during early drug development using hERG inhibition and an anaesthetized guinea-pig model. British Journal of Pharmacology. 2008;154(7):1446-56.

20. Chain A, Sturkenboom M, Danhof M, Pasqua OD. Establishing< i> in vitro</i> to clinical correlations in the evaluation of cardiovascular safety pharmacology. Drug Discovery Today: Technologies. 2012.

21. Pollard C, Valentin JP, Hammond T. Strategies to reduce the risk of drug-induced QT interval prolongation: a pharmaceutical company perspective. British Journal of Pharmacology. 2008;154(7):1538-43.

22. Polak S, Pugsley MK, Stockbridge N, Garnett C, Wisniowska B. Early Drug Discovery Prediction of Proarrhythmia Potential and Its Covariates. AAPS J. 2015;17(4):1025-32. doi: 10.1208/s12248-015-9773-1.

23. Patel N, Hatley O, Berg A, Romero K, Wisniowska B, Hanna D, et al. Towards Bridging Translational Gap in Cardiotoxicity Prediction: an Application of Progressive Cardiac Risk Assessment Strategy in TdP Risk Assessment of Moxifloxacin. AAPS J. 2018;20(3):47. doi: 10.1208/s12248-018-0199-4.

24. Hondeghem LM. Drug-Induced QT Prolongation and Torsades de Pointes: An All-Exclusive Relationship or Time for an Amicable Separation? Drug Saf. 2018;41(1):11-7. doi: 10.1007/s40264-017-0584-4.

25. Overø K, Hojelse F, editors. The unexpected preclinical finding-elucidation of dog toxicity-citalopram. Proceedings of the Association of the Swedish Pharmaceutical Industry workshop on the use of pharmacology studies in drug safety assessment-present situation and future perspectives 1994 26-27 Sept; Stockholm, Sweden1994.

26. Patel N, Wiśniowska B, Jamei M, Polak S. Real Patient and its Virtual Twin: Application of Quantitative Systems Toxicology Modelling in the Cardiac Safety Assessment of Citalopram. The AAPS Journal. 2017;20(1):6. doi: 10.1208/s12248-017-0155-8.

27. Patel N, Wisniowska B, Polak S. Virtual Thorough QT (TQT) Trial-Extrapolation of In Vitro Cardiac Safety Data to In Vivo Situation Using Multi-Scale Physiologically Based Ventricular Cell-wall Model Exemplified with Tolterodine and Fesoterodine. AAPS J. 2018;20(5):83. doi: 10.1208/s12248-018-0244-3.

28. Polak S, Romero K, Berg A, Patel N, Jamei M, Hermann D, et al. Quantitative Approach for Cardiac Risk Assessment and Interpretation in Tuberculosis Drug Development. Journal of Pharmacokinetics and Pharmacodynamics. 2017.

29. Polak S, Wisniowska B, Fijorek K, Glinka A, Mendyk A. In vitro-in vivo extrapolation of drug-induced proarrhythmia predictions at the population level. Drug Discov Today. 2014;19(3):275-81. doi: 10.1016/j.drudis.2013.10.009S1359-6446(13)00335-8 [pii].

30. Polak S, Wisniowska B, Fijorek K, Glinka A, Polak M, Mendyk A, editors. ToxComp┼ In vitro-in vivo extrapolation system for drug proarrhythmic potency assessment. Computing in Cardiology (CinC), 2012; 2012: IEEE.

31. Abbasi M, Small BG, Patel N, Jamei M, Polak S. Early assessment of proarrhythmic risk of drugs using the in vitro data and single-cell-based in silico models: proof of concept. Toxicol Mech Methods. 2016:1-12. doi: 10.1080/15376516.2016.1256460.

32. Fijorek K, Patel N, Klima Ł, Stolarz-Skrzypek K, Kawecka-Jaszcz K, Polak S. Age and gender dependent heart rate circadian model development and performance verification on the proarrhythmic drug case study. Theoretical Biology and Medical Modelling. 2013;10(1):7.

33. Goldberger AL, Amaral LAN, Glass L, Hausdorff JM, Ivanov PC, Mark RG, et al. PhysioBank, PhysioToolkit, and PhysioNet: components of a new research resource for complex physiologic signals. Circulation. 2000;101. doi: 10.1161/01.CIR.101.23.e215.

34. ten Tusscher KH, Panfilov AV. Alternans and spiral breakup in a human ventricular tissue model. Am J Physiol Heart Circ Physiol. 2006;291(3):H1088-100. doi: 00109.2006 [pii]10.1152/ajpheart.00109.2006.

35. Polak S, Fijorek K. Inter-individual Variability in the Pre-clinical Drug Cardiotoxic Safety Assessment—Analysis of the Age–Cardiomyocytes Electric Capacitance Dependence. Journal of cardiovascular translational research. 2012;5(3):321-32.

36. Polak S, Fijorek K, Glinka A, Wisniowska B, Mendyk A. Virtual population generator for human cardiomyocytes parameters: in silico drug cardiotoxicity assessment. Toxicology Mechanisms and Methods. 2012;22(1):31-40.

37. Grosjean P, Urien S. Reevaluation of moxifloxacin in pharmacokinetics and their direct effect on the QT interval. J Clin Pharmacol. 2012;52. doi: 10.1177/0091270011398361.

38. Stass H, Kubitza D, Schuhly U. Pharmacokinetics, safety and tolerability of moxifloxacin, a novel 8-methoxyfluoroquinolone, after repeated oral administration. Clin Pharmacokinet. 2001;40 Suppl 1:1-9.

39. Polak S, Wisniowska B, Glinka A, Polak M. Tox-database.net: a curated resource for data describing chemical triggered in vitro cardiac ion channels inhibition. BMC Pharmacol Toxicol. 2012;13:6. doi: 10.1186/2050-6511-13-62050-6511-13-6 [pii].

40. Alexandrou AJ, Duncan RS, Sullivan A, Hancox JC, Leishman DJ, Witchel HJ, et al. Mechanism of hERG K+ channel blockade by the fluoroquinolone antibiotic moxifloxacin. Br J Pharmacol. 2006;147(8):905-16. doi: 10.1038/sj.bjp.0706678.

41. Malhotra BK, Glue P, Sweeney K, Anziano R, Mancuso J, Wicker P. Thorough QT study with recommended and supratherapeutic doses of tolterodine. Clin Pharmacol Ther. 2007;81(3):377-85. doi: 10.1038/sj.clpt.6100089.

42. Oishi M, Chiba K, Malhotra B, Suwa T. Effect of the CYP2D6*10 genotype on tolterodine pharmacokinetics. Drug Metab Dispos. 2010;38(9):1456-63. doi: 10.1124/dmd.110.033407.

43. Mizutani T. PM frequencies of major CYPs in Asians and Caucasians. Drug Metab Rev. 2003;35(2-3):99-106. doi: 10.1081/DMR-120023681.

44. Malhotra B, Gandelman K, Sachse R, Wood N, Michel MC. The design and development of fesoterodine as a prodrug of 5-hydroxymethyl tolterodine (5-HMT), the active metabolite of tolterodine. Curr Med Chem. 2009;16(33):4481-9.

45. Malhotra B, Wood N, Sachse R, Gandelman K. Thorough QT study of the effect of fesoterodine on cardiac repolarization. Int J Clin Pharmacol Ther. 2010;48(5):309-18.

46. Brynne N, Dalen P, Alvan G, Bertilsson L, Gabrielsson J. Influence of CYP2D6 polymorphism on the pharmacokinetics and pharmacodynamic of tolterodine. Clin Pharmacol Ther. 1998;63(5):529-39. doi: 10.1016/S0009-9236(98)90104-7.

47. Malhotra B, Dickins M, Alvey C, Jumadilova Z, Li X, Duczynski G, et al. Effects of the moderate CYP3A4 inhibitor, fluconazole, on the pharmacokinetics of fesoterodine in healthy subjects. Br J Clin Pharmacol. 2011;72(2):263-9. doi: 10.1111/j.1365-2125.2011.04007.x.

48. Okada J, Yoshinaga T, Kurokawa J, Washio T, Furukawa T, Sawada K, et al. Screening system for drug-induced arrhythmogenic risk combining a patch clamp and heart simulator. Sci Adv. 2015;1(4):e1400142. doi: 10.1126/sciadv.1400142.

49. .

50. Jamei M, Marciniak S, Edwards D, Wragg K, Feng K, Barnett A, et al. The simcyp population based simulator: architecture, implementation, and quality assurance. In Silico Pharmacol. 2013;1:9. doi: 10.1186/2193-9616-1-99 [pii].

51. Patel N, Polak S, Jamei M, Rostami-Hodjegan A, Turner DB. Quantitative prediction of formulation-specific food effects and their population variability from in vitro data with the physiologically-based ADAM model: a case study using the BCS/BDDCS Class II drug nifedipine. Eur J Pharm Sci. 2014;57:240-9. doi: 10.1016/j.ejps.2013.09.006.

52. Jamei M, Turner D, Yang J, Neuhoff S, Polak S, Rostami-Hodjegan A, et al. Population-based mechanistic prediction of oral drug absorption. AAPS J. 2009;11(2):225-37. doi: 10.1208/s12248-009-9099-y.

53. Hatley OJ, Patel N, Gaohua L, Burt H, Neuhoff S, Romero K, et al., editors. Application of a multi-compartment permeability-limited lung model to predict lung concentrations of moxifloxacin in virtual human subjects. DRUG METABOLISM REVIEWS; 2016: TAYLOR & FRANCIS LTD 2-4 PARK SQUARE, MILTON PARK, ABINGDON OR14 4RN, OXON, ENGLAND.

54. Poulin P, Theil FP. Prediction of pharmacokinetics prior to in vivo studies. 1. Mechanism-based prediction of volume of distribution. J Pharm Sci. 2002;91(1):129-56.

55. Berezhkovskiy LM. Volume of distribution at steady state for a linear pharmacokinetic system with peripheral elimination. J Pharm Sci. 2004;93(6):1628-40. doi: 10.1002/jps.20073.

56. Polonchuk L. Toward a New Gold Standard for Early Safety: Automated Temperature-Controlled hERG Test on the PatchLiner. Front Pharmacol. 2012;3:3. doi: 10.3389/fphar.2012.00003.

57. Langlois MH, Montagut M, Dubost JP, Grellet J, Saux MC. Protonation equilibrium and lipophilicity of moxifloxacin. J Pharm Biomed Anal. 2005;37(2):389-93. doi: S0731-7085(04)00544-8 [pii]10.1016/j.jpba.2004.10.022.

58. Muller M, Stass H, Brunner M, Moller JG, Lackner E, Eichler HG. Penetration of moxifloxacin into peripheral compartments in humans. Antimicrob Agents Chemother. 1999;43(10):2345-9.

59. Siefert HM, Domdey-Bette A, Henninger K, Hucke F, Kohlsdorfer C, Stass HH. Pharmacokinetics of the 8-methoxyquinolone, moxifloxacin: a comparison in humans and other mammalian species. J Antimicrob Chemother. 1999;43 Suppl B:69-76.

60. Stass H, Dalhoff A, Kubitza D, Schuhly U. Pharmacokinetics, safety, and tolerability of ascending single doses of moxifloxacin, a new 8-methoxy quinolone, administered to healthy subjects. Antimicrob Agents Chemother. 1998;42(8):2060-5.

61. Stass H, Kubitza D. Pharmacokinetics and elimination of moxifloxacin after oral and intravenous administration in man. J Antimicrob Chemother. 1999;43 Suppl B:83-90.

62. Vu DH, Koster RA, Alffenaar JW, Brouwers JR, Uges DR. Determination of moxifloxacin in dried blood spots using LC-MS/MS and the impact of the hematocrit and blood volume. J Chromatogr B Analyt Technol Biomed Life Sci. 2011;879(15-16):1063-70. doi: 10.1016/j.jchromb.2011.03.017S1570-0232(11)00164-4 [pii].

63. Kim SH, Jung SJ, S.Y. U, VNa MA, Choi MJ, Chung MW, et al. Effect of Cimetidine on the Transport of Quinolone Antibiotics in Caco-2 Cell monolayers. J Applied Pharmacol. 2007;15:102-7.

64. Stass H, Bottcher MF, Ochmann K. Evaluation of the influence of antacids and H2 antagonists on the absorption of moxifloxacin after oral administration of a 400mg dose to healthy volunteers. Clin Pharmacokinet. 2001;40 Suppl 1:39-48.

65. Stass H, Kubitza D. Lack of pharmacokinetic interaction between moxifloxacin, a novel 8-methoxyfluoroquinolone, and theophylline. Clin Pharmacokinet. 2001;40 Suppl 1:63-70.

66. Stass H, Nagelschmitz J, Moeller JG, Delesen H. Pharmacokinetics of moxifloxacin are not influenced by a 7-day pretreatment with 200 mg oral itraconazole given once a day in healthy subjects. Int J Clin Pharmacol Ther. 2004;42(1):23-9.

67. Polak S, Fijorek K, Püsküllüoğlu M, Glinka A, Tomaszewska D, Tomaszewski R. Literature review of the serum potassium, sodium and calcium levels in healthy individuals. 2013.

68. Sennels HP, Jørgensen HL, Goetze JP, Fahrenkrug J. Rhythmic 24-hour variations of frequently used clinical biochemical parameters in healthy young males-The Bispebjerg study of diurnal variations. Scandinavian Journal of Clinical & Laboratory Investigation. 2012;72(4):287-95.

69. O'Hara T, Virag L, Varro A, Rudy Y. Simulation of the undiseased human cardiac ventricular action potential: model formulation and experimental validation. PLoS Comput Biol. 2011;7(5):e1002061. doi: 10.1371/journal.pcbi.1002061.

70. Anderson ME, Mazur A, Yang T, Roden DM. Potassium current antagonist properties and proarrhythmic consequences of quinolone antibiotics. J Pharmacol Exp Ther. 2001;296(3):806-10.

71. Bischoff U, Schmidt C, Netzer R, Pongs O. Effects of fluoroquinolones on HERG currents. Eur J Pharmacol. 2000;406(3):341-3.

72. Champeroux P, Ouille A, Martel E, Fowler JS, Maurin A, Richard S, et al. A step towards characterisation of electrophysiological profile of torsadogenic drugs. J Pharmacol Toxicol Methods. 2011;63(3):269-78. doi: 10.1016/j.vascn.2011.01.001.

73. Chen X, Cass JD, Bradley JA, Dahm CM, Sun Z, Kadyszewski E, et al. QT prolongation and proarrhythmia by moxifloxacin: concordance of preclinical models in relation to clinical outcome. Br J Pharmacol. 2005;146(6):792-9. doi: 10.1038/sj.bjp.0706389.

74. Eichenbaum G, Pugsley MK, Gallacher DJ, Towart R, McIntyre G, Shukla U, et al. Role of mixed ion channel effects in the cardiovascular safety assessment of the novel anti-MRSA fluoroquinolone JNJ-Q2. Br J Pharmacol. 2012;166(5):1694-707. doi: 10.1111/j.1476-5381.2012.01874.x.

75. Kang J, Wang L, Chen XL, Triggle DJ, Rampe D. Interactions of a series of fluoroquinolone antibacterial drugs with the human cardiac K+ channel HERG. Mol Pharmacol. 2001;59(1):122-6.

76. Kramer J, Obejero-Paz CA, Myatt G, Kuryshev YA, Bruening-Wright A, Verducci JS, et al. MICE models: superior to the HERG model in predicting Torsade de Pointes. Sci Rep. 2013;3:2100. doi: 10.1038/srep02100.

77. Lacroix P, Crumb WJ, Durando L, Ciottoli GB. Prulifloxacin: in vitro (HERG current) and in vivo (conscious dog) assessment of cardiac risk. Eur J Pharmacol. 2003;477(1):69-72.

78. Lu HR, Vlaminckx E, Van de Water A, Rohrbacher J, Hermans A, Gallacher DJ. In-vitro experimental models for the risk assessment of antibiotic-induced QT prolongation. Eur J Pharmacol. 2006;553(1-3):229-39. doi: 10.1016/j.ejphar.2006.09.035.

79. Mannikko R, Overend G, Perrey C, Gavaghan CL, Valentin JP, Morten J, et al. Pharmacological and electrophysiological characterization of nine, single nucleotide polymorphisms of the hERG-encoded potassium channel. Br J Pharmacol. 2010;159(1):102-14. doi: 10.1111/j.1476-5381.2009.00334.x.

80. Martin RL, McDermott JS, Salmen HJ, Palmatier J, Cox BF, Gintant GA. The utility of hERG and repolarization assays in evaluating delayed cardiac repolarization: influence of multi-channel block. J Cardiovasc Pharmacol. 2004;43(3):369-79.

81. Mirams GR, Davies MR, Brough SJ, Bridgland-Taylor MH, Cui Y, Gavaghan DJ, et al. Prediction of Thorough QT study results using action potential simulations based on ion channel screens. J Pharmacol Toxicol Methods. 2014;70(3):246-54. doi: 10.1016/j.vascn.2014.07.002.

82. Thomsen MB, Beekman JD, Attevelt NJ, Takahara A, Sugiyama A, Chiba K, et al. No proarrhythmic properties of the antibiotics Moxifloxacin or Azithromycin in anaesthetized dogs with chronic-AV block. Br J Pharmacol. 2006;149(8):1039-48. doi: 10.1038/sj.bjp.0706900.

83. Yao X, Anderson DL, Ross SA, Lang DG, Desai BZ, Cooper DC, et al. Predicting QT prolongation in humans during early drug development using hERG inhibition and an anaesthetized guinea-pig model. Br J Pharmacol. 2008;154(7):1446-56. doi: 10.1038/bjp.2008.267.

84. Liotier J, Coudore F. Drug monitoring of a case of citalopram overdosage. Drug Chem Toxicol. 2011;34(4):420-3. doi: 10.3109/01480545.2011.566571.

85. Tarabar AF, Hoffman RS, Nelson L. Citalopram overdose: late presentation of torsades de pointes (TdP) with cardiac arrest. J Med Toxicol. 2008;4(2):101-5.

86. Unterecker S, Warrings B, Deckert J, Pfuhlmann B. Correlation of QTc interval prolongation and serum level of citalopram after intoxication--a case report. Pharmacopsychiatry. 2012;45(1):30-4. doi: 10.1055/s-0031-1286346.

87. US Food and Drug Adminstration. FDA Drug Safety Communication: Abnormal heart rhythms associated with high doses of Celexa (citalopram hydrobromide). Silver Spring, MD: US Food and Drug Adminstration; 2011.

88. Ji Y, Schaid DJ, Desta Z, Kubo M, Batzler AJ, Snyder K, et al. Citalopram and escitalopram plasma drug and metabolite concentrations: genome-wide associations. Br J Clin Pharmacol. 2014;78(2):373-83. doi: 10.1111/bcp.12348.

89. Jamei M, Marciniak S, Feng K, Barnett A, Tucker G, Rostami-Hodjegan A. The Simcyp population-based ADME simulator. Expert Opin Drug Metab Toxicol. 2009;5(2):211-23. doi: 10.1517/17425250802691074 [pii].

90. Lobell M, Sivarajah V. In silico prediction of aqueous solubility, human plasma protein binding and volume of distribution of compounds from calculated pKa and AlogP98 values. Mol Divers. 2003;7(1):69-87.

91. Baumann P, Larsen F. The Pharmacokinetics of Citalopram. Rev Contemp Pharmaco. 1995;6:287-95.

92. US Food and Drug Adminstration. FDA Drug Safety Communication: Revised Recommendations for Celexa (citalopram hydrobromide) Related to a Potential Risk of Abnormal Heart Rhythms with High Doses. Silver Spring, MD: US Food and Drug Adminstration; 2012.

93. Wisniowska B, Polak S. The Role of Interaction Model in Simulation of Drug Interactions and QT Prolongation. Curr Pharmacol Rep. 2016;2(6):339-44. doi: 10.1007/s40495-016-0075-975 [pii].

94. Rohrbacher J, Bex P, Gallacher DJ. Citalopram metabolites inhibit IKs and IKr differentially: Is this a possible explanation for the sudden deaths in dogs? J Pharmacol Toxicol Meth. 2012;66(2):170. doi: 10.1016/j.vascn.2012.08.040.

95. Hamplova-Peichlova J, Krusek J, Paclt I, Slavicek J, Lisa V, Vyskocil F. Citalopram inhibits L-type calcium channel current in rat cardiomyocytes in culture. Physiol Res. 2002;51(3):317-21.

96. Polak S, Fijorek K. Inter-individual variability in the pre-clinical drug cardiotoxic safety assessment--analysis of the age-cardiomyocytes electric capacitance dependence. J Cardiovasc Transl Res. 2012;5(3):321-32. doi: 10.1007/s12265-012-9357-8.

97. Fijorek K, Puskulluoglu M, Polak S. Circadian models of serum potassium, sodium, and calcium concentrations in healthy individuals and their application to cardiac electrophysiology simulations at individual level. Comput Math Methods Med. 2013;2013:429037. doi: 10.1155/2013/429037.

98. Aschoff J. Circadian Rhythms in Man. A self-sustained oscillator with an inherent frequency underlies human 24-hour periodicity. Science. 1965;148. doi: 10.1126/science.148.3676.1427.

99. Kanabrocki EL, Sothern RB, Scheving LE, Vesely DL, Tsai TH, Shelstad J, et al. Reference values for circadian rhythms of 98 variables in clinically healthy men in the fifth decade of life. Chronobiol Int. 1990;7. doi: 10.3109/07420529009059156.

100. Piotrovsky V. Pharmacokinetic-pharmacodynamic modeling in the data analysis and interpretation of drug-induced QT/QTc prolongation. AAPS J. 2005;7. doi: 10.1208/aapsj070363.

101. Nakagawa M, Iwao T, Ishida S, Yonemochi H, Fujino T, Saikawa T, et al. Circadian rhythm of the signal averaged electrocardiogram and its relation to heart rate variability in healthy subjects. Heart. 1998;79. doi: 10.1136/hrt.79.5.493.

102. Li X, Shaffer ML, Rodriguez-Colon S, He F, Wolbrette DL, Alagona P, et al. The circadian pattern of cardiac autonomic modulation in a middle-aged population. Clin Auton Res. 2011;21. doi: 10.1007/s10286-010-0112-4.

103. Massin MM, Maeyns K, Withofs N, Ravet F, Gerard P. Circadian rhythm of heart rate and heart rate variability. Arch Dis Child. 2000;83. doi: 10.1136/adc.83.2.179.

104. Bonnemeier H, Richardt G, Potratz J, Wiegand UK, Brandes A, Kluge N, et al. Circadian Profile of Cardiac Autonomic Nervous Modulation in Healthy Subjects: Differing Effects of Aging and Gender on Heart Rate Variability. J Cardiovasc Electrophysiol. 2003;14. doi: 10.1046/j.1540-8167.2003.03078.x.

105. Cavallari JM, Fang SC, Mittleman MA, Christiani DC. Circadian variation of heart rate variability among welders. Occup Environ Med. 2010;67. doi: 10.1136/oem.2010.055210.

106. Cugini P, Bernardini F, Cardarello CM, Coda S, Curione M, De Francesco GP, et al. Circadian rhythm of heart rate in myotonic dystrophy. J Clin Basic Cardiol. 2000;3.

107. D'Negri CE, Marelich L, Vigo D, Acunzo RS, Girotti LA, Cardinali DP, et al. Circadian periodicity of heart rate variability in hospitalized angor patients. Clin Auton Res. 2005;15. doi: 10.1007/s10286-005-0280-9.

108. Eisenbruch S, Harnish MJ, Orr WC. Heart rate variability during waking and sleep in healthy males and females. Sleep. 1999;22.

109. Garnett C, Beasley N, Bhattaram VA, Jadhav PR, Madabushi R, Stockbridge N, et al. Concentration-QT relationships play a key role in the evaluation of proarrhythmic risk during regulatory review. J Clin Pharmacol. 2008;48. doi: 10.1177/0091270007307881.

110. Sweeney KR, Gastonguay MR, Benincosa L, Cronenberger CL, Glue P, Malhotra BK. Exposure-response modeling and clinical trial simulation of the effect of tolterodine on QT intervals in healthy volunteers. Drug Discov Ther. 2010;4(1):44-53.

111. Florian JA, Tornoe CW, Brundage R, Parekh A, Garnett CE. Population pharmacokinetic and concentration--QTc models for moxifloxacin: pooled analysis of 20 thorough QT studies. J Clin Pharmacol. 2011;51(8):1152-62. doi: 10.1177/0091270010381498.

112. Bloomfield DM, Kost JT, Ghosh K, Hreniuk D, Hickey LA, Guitierrez MJ, et al. The effect of moxifloxacin on QTc and implications for the design of thorough QT studies. Clin Pharmacol Ther. 2008;84(4):475-80.

113. Kligfield P, Green CL, Mortara J, Sager P, Stockbridge N, Li M, et al. The Cardiac Safety Research Consortium electrocardiogram warehouse: thorough QT database specifications and principles of use for algorithm development and testing. Am Heart J. 2010;160(6):1023-8. doi: 10.1016/j.ahj.2010.09.002.

114. Morganroth J, Wang Y, Thorn M, Kumagai Y, Harris S, Stockbridge N, et al. Moxifloxacin-induced QTc interval prolongations in healthy male Japanese and Caucasian volunteers: a direct comparison in a thorough QT study. Br J Clin Pharmacol. 2015;80(3):446-59. doi: 10.1111/bcp.12684.

115. Panicker GK, Karnad DR, Kadam P, Badilini F, Damle A, Kothari S. Detecting moxifloxacin-induced QTc prolongation in thorough QT and early clinical phase studies using a highly automated ECG analysis approach. Br J Pharmacol. 2016;173(8):1373-80. doi: 10.1111/bph.13436.

116. Taubel J, Ferber G, Lorch U, Batchvarov V, Savelieva I, Camm AJ. Thorough QT study of the effect of oral moxifloxacin on QTc interval in the fed and fasted state in healthy Japanese and Caucasian subjects. Br J Clin Pharmacol. 2014;77(1):170-9. doi: 10.1111/bcp.12168.

117. Zhang X, Silkey M, Schumacher M, Wang L, Raval H, Caulfield JP. Period correction of the QTc of moxifloxacin with multiple predose baseline ECGs is the least variable of 4 methods tested. J Clin Pharmacol. 2009;49(5):534-9. doi: 10.1177/0091270008330158.

118. Altin T, Ozcan O, Turhan S, Ongun Ozdemir A, Akyurek O, Karaoguz R, et al. Torsade de pointes associated with moxifloxacin: a rare but potentially fatal adverse event. Can J Cardiol. 2007;23(11):907-8.

119. Chetty M, Rose RH, Abduljalil K, Patel N, Lu G, Cain T, et al. Applications of linking PBPK and PD models to predict the impact of genotypic variability, formulation differences, differences in target binding capacity and target site drug concentrations on drug responses and variability. Front Pharmacol. 2014;5:258. doi: 10.3389/fphar.2014.00258.

120. Rose RH, Neuhoff S, Abduljalil K, Chetty M, Rostami-Hodjegan A, Jamei M. Application of a Physiologically Based Pharmacokinetic Model to Predict OATP1B1-Related Variability in Pharmacodynamics of Rosuvastatin. CPT Pharmacometrics Syst Pharmacol. 2014;3:e124. doi: 10.1038/psp.2014.24.

121. Minematsu T, Ohtani H, Yamada Y, Sawada Y, Sato H, Iga T. Quantitative relationship between myocardial concentration of tacrolimus and QT prolongation in guinea pigs: pharmacokinetic/pharmacodynamic model incorporating a site of adverse effect. J Pharmacokinet Pharmacodyn. 2001;28(6):533-54.

122. Melgari D, Zhang Y, El Harchi A, Dempsey CE, Hancox JC. Molecular basis of hERG potassium channel blockade by the class Ic antiarrhythmic flecainide. J Mol Cell Cardiol. 2015;86:42-53. doi: 10.1016/j.yjmcc.2015.06.021.

123. Zhang S, Rajamani S, Chen Y, Gong Q, Rong Y, Zhou Z, et al. Cocaine blocks HERG, but not KvLQT1+minK, potassium channels. Mol Pharmacol. 2001;59(5):1069-76.

124. Onohara T, Hisatome I, Kurata Y, Li P, Notsu T, Morikawa K, et al. Molecular mechanisms underlying the pilsicainide-induced stabilization of hERG proteins in transfected mammalian cells. J Arrhythm. 2017;33(3):226-33. doi: 10.1016/j.joa.2016.09.003.

125. Tylutki Z, Mendyk A, Polak S. Mechanistic Physiologically Based Pharmacokinetic (PBPK) Model of the Heart Accounting for Inter-individual Variability: Development and Performance Verification. J Pharm Sci. 2017. doi: 10.1016/j.xphs.2017.11.012.

126. Tylutki Z, Polak S. A four-compartment PBPK heart model accounting for cardiac metabolism - model development and application. Sci Rep. 2017;7:39494. doi: 10.1038/srep39494.

127. Shah RR. Drug-induced QT interval prolongation: does ethnicity of the thorough QT study population matter? Br J Clin Pharmacol. 2013;75(2):347-58. doi: 10.1111/j.1365-2125.2012.04415.x.

128. Sager PT, Gintant G, Turner JR, Pettit S, Stockbridge N. Rechanneling the cardiac proarrhythmia safety paradigm: a meeting report from the Cardiac Safety Research Consortium. Am Heart J. 2014;167(3):292-300. doi: 10.1016/j.ahj.2013.11.004.

129. Badshah A, Janjua M, Younas F, Halabi AR, Cotant JF. Moxifloxacin-induced QT prolongation and torsades: an uncommon effect of a common drug. Am J Med Sci. 2009;338(2):164-6. doi: 10.1097/MAJ.0b013e3181a3c2c9.

130. Sherazi S, DiSalle M, Daubert JP, Shah AH. Moxifloxacin-induced torsades de pointes. Cardiol J. 2008;15(1):71-3.

131. Bohm R, Hocker J, Cascorbi I, Herdegen T. OpenVigil--free eyeballs on AERS pharmacovigilance data. Nat Biotechnol. 2012;30(2):137-8. doi: 10.1038/nbt.2113.

132. Elkins RC, Davies MR, Brough SJ, Gavaghan DJ, Cui Y, Abi-Gerges N, et al. Variability in high-throughput ion-channel screening data and consequences for cardiac safety assessment. Journal of Pharmacological and Toxicological Methods. 2013.

133. Wisniowska B, Polak S. hERG in vitro interchange factors-development and verification. Toxicology Mechanisms and Methods. 2009;19(4):278-84.

134. Li Z, Dutta S, Sheng J, Tran PN, Wu W, Chang K, et al. Improving the In Silico Assessment of Proarrhythmia Risk by Combining hERG (Human Ether-a-go-go-Related Gene) Channel-Drug Binding Kinetics and Multichannel Pharmacology. Circ Arrhythm Electrophysiol. 2017;10(2):e004628. doi: 10.1161/CIRCEP.116.004628.

135. Friesen KJ, Bugden SC. The effectiveness and limitations of regulatory warnings for the safe prescribing of citalopram. Drug Healthc Patient Saf. 2015;7:139-45. doi: 10.2147/DHPS.S91046dhps-7-139 [pii].

136. Witchel HJ, Pabbathi VK, Hofmann G, Paul AA, Hancox JC. Inhibitory actions of the selective serotonin re-uptake inhibitor citalopram on HERG and ventricular L-type calcium currents. FEBS Lett. 2002;512(1-3):59-66. doi: S0014579301033208 [pii].

137. Pacher P, Ungvari Z, Nanasi PP, Furst S, Kecskemeti V. Speculations on difference between tricyclic and selective serotonin reuptake inhibitor antidepressants on their cardiac effects. Is there any? Curr Med Chem. 1999;6(6):469-80.

138. Friberg LE, Isbister GK, Duffull SB. Pharmacokinetic-pharmacodynamic modelling of QT interval prolongation following citalopram overdoses. Br J Clin Pharmacol. 2006;61(2):177-90. doi: BCP2546 [pii]10.1111/j.1365-2125.2005.02546.x.

139. Bird ST, Crentsil V, Temple R, Pinheiro S, Demczar D, Stone M. Cardiac safety concerns remain for citalopram at dosages above 40 mg/day. Am J Psychiatry. 2014;171(1):17-9. doi: 10.1176/appi.ajp.2013.130709051809635 [pii].

140. Zivin K, Pfeiffer PN, Bohnert AS, Ganoczy D, Blow FC, Nallamothu BK, et al. Evaluation of the FDA warning against prescribing citalopram at doses exceeding 40 mg. Am J Psychiatry. 2013;170(6):642-50. doi: 10.1176/appi.ajp.2013.120304081685280 [pii].

141. Hutton LM, Cave AJ, St-Jean R, Banh HL. Should We be Worried About QTc Prolongation Using Citalopram? A Review. J Pharm Pract. 2016;30(3):353-8. doi: 0897190015624862 [pii]10.1177/0897190015624862.

142. Wisniowska B, Polak S. Virtual Clinical Trial Toward Polytherapy Safety Assessment: Combination of Physiologically Based Pharmacokinetic/Pharmacodynamic-Based Modeling and Simulation Approach With Drug-Drug Interactions Involving Terfenadine as an Example. J Pharm Sci. 2016;105(11):3415-24. doi: S0022-3549(16)41634-5 [pii]10.1016/j.xphs.2016.08.002.

143. Wisniowska B, Polak S. Am I or am I not proarrhythmic? Comparison of various classifications of drug TdP propensity. Drug Discov Today. 2017;22(1):10-6. doi: S1359-6446(16)30372-5 [pii]10.1016/j.drudis.2016.09.027.

144. Colatsky T, Fermini B, Gintant G, Pierson JB, Sager P, Sekino Y, et al. The Comprehensive in Vitro Proarrhythmia Assay (CiPA) initiative - Update on progress. J Pharmacol Toxicol Methods. 2016;81:15-20. doi: 10.1016/j.vascn.2016.06.002S1056-8719(16)30058-2 [pii].

145. Crumb WJ, Jr., Vicente J, Johannesen L, Strauss DG. An evaluation of 30 clinical drugs against the comprehensive in vitro proarrhythmia assay (CiPA) proposed ion channel panel. J Pharmacol Toxicol Methods. 2016;81:251-62. doi: 10.1016/j.vascn.2016.03.009S1056-8719(16)30017-X [pii].

146. Cavero I, Guillon JM, Ballet V, Clements M, Gerbeau JF, Holzgrefe H. Comprehensive in vitro Proarrhythmia Assay (CiPA): Pending issues for successful validation and implementation. J Pharmacol Toxicol Methods. 2016;81:21-36. doi: 10.1016/j.vascn.2016.05.012S1056-8719(16)30052-1 [pii].

147. Wisniowska B, Tylutki Z, Wyszogrodzka G, Polak S. Drug-drug interactions and QT prolongation as a commonly assessed cardiac effect - comprehensive overview of clinical trials. BMC Pharmacol Toxicol. 2016;17:12. doi: 10.1186/s40360-016-0053-110.1186/s40360-016-0053-1 [pii].

148. Tucker GT, Rostami-Hodjegan A, Toon S. Systems and methods for predicting and adjusting the dosage of medicines in individual patients. In: Office USPaT, editor.: Google Patents.

149. Segal NL, McGuire SA, Stohs JH. What Virtual Twins Reveal About General Intelligence and Other Behaviors. Personality and individual differences. 2012;53:405-10. doi: 10.1016/j.paid.2011.11.019.

150. Bedding A, Scott G, Brayshaw N, Leong L, Herrero-Martinez E, Looby M, et al. Clinical trial simulations–an essential tool in drug development. ABPI2014. p. 1-15.

151. Hartmanshenn C, Scherholz M, Androulakis IP. Physiologically-based pharmacokinetic models: approaches for enabling personalized medicine. J Pharmacokinet Pharmacodyn. 2016;43(5):481-504. doi: 10.1007/s10928-016-9492-y10.1007/s10928-016-9492-y [pii].

152. Jamei M. Recent Advances in Development and Application of Physiologically-Based Pharmacokinetic (PBPK) Models: a Transition from Academic Curiosity to Regulatory Acceptance. Curr Pharmacol Rep. 2016;2:161-9. doi: 10.1007/s40495-016-0059-959 [pii].

153. Tucker GT. Personalized Drug Dosage - Closing the Loop. Pharm Res. 2017;34(8):1539-43. doi: 10.1007/s11095-016-2076-010.1007/s11095-016-2076-0 [pii].

154. Bazett HC. An analysis of the time-relations of electrocardiograms. Annals of Noninvasive Electrocardiology. 1997;2:177-94. doi: 10.1111/j.1542-474X.1997.tb00325.x.

155. Tylutki Z, Polak S. Plasma vs heart tissue concentration in humans - literature data analysis of drugs distribution. Biopharm Drug Dispos. 2015;36(6):337-51. doi: 10.1002/bdd.1944.

Appendix

Publications appended in following order

P-I

P-II

P-III

P-IV